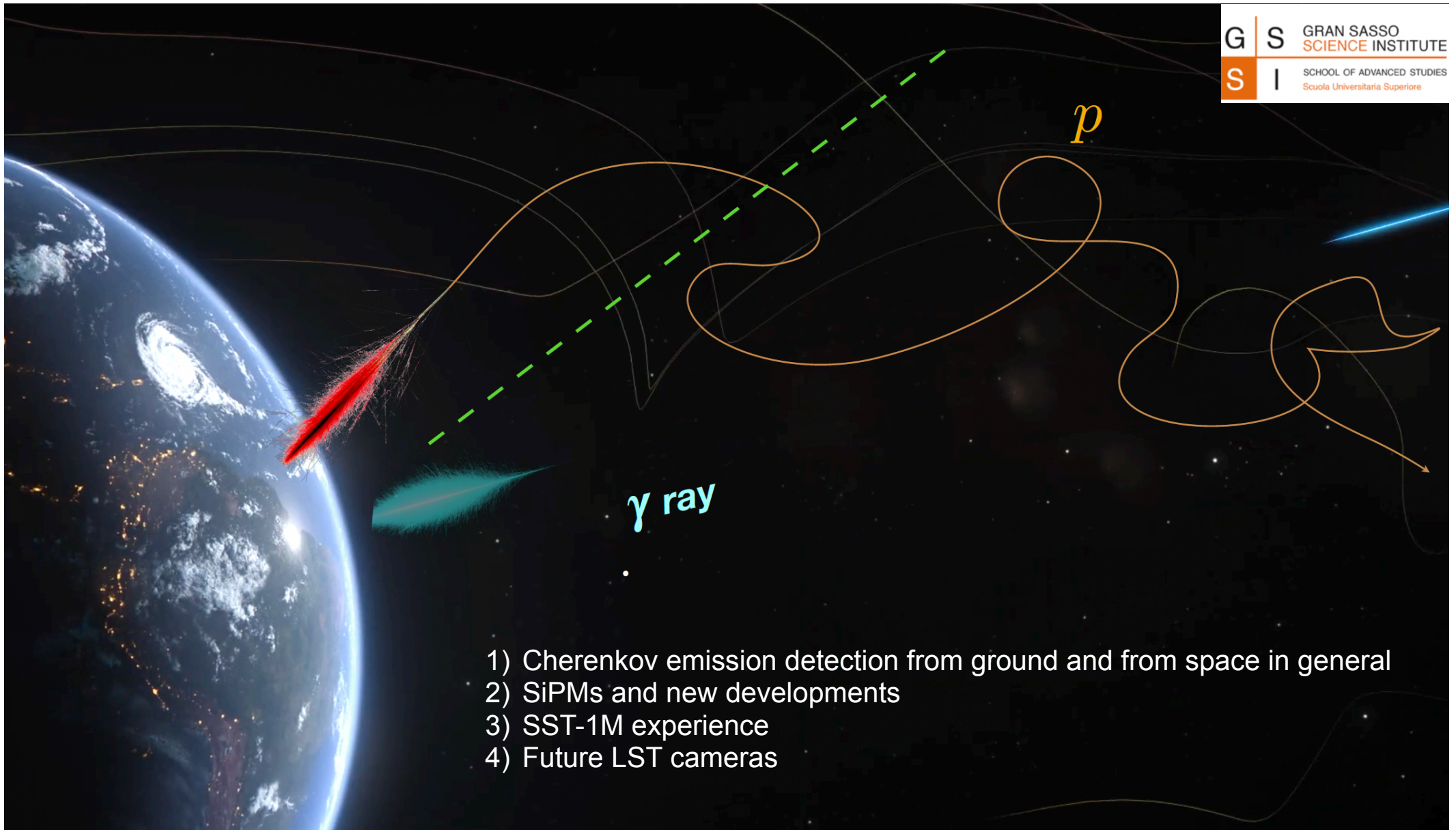


# The application of SiPM for Cherenkov light detection in the atmosphere



- 1) Cherenkov emission detection from ground and from space in general
- 2) SiPMs and new developments
- 3) SST-1M experience
- 4) Future LST cameras

# The atmospheric calorimeter



The atmosphere is a calorimeter of  $\sim 27X_0$   
 The radiation length characterises radiative energy losses due to bremsstrahlung:

$X_0 \sim 37\text{gcm}^{-2}$  ( $\sim 300$  m a.s.l., 1km at 10 km of altitude)

Pair production  $L_{ee} = 9/7X_0$

For  $E \gg E_c \sim \alpha X_0 \sim 83$  MeV  
 $E \propto E_0 e^{(-X/X_0)}$  and  $E = E_0/2$  in

$$\ell = \ln 2 X_0 \sim 25\text{gcm}^{-2}$$

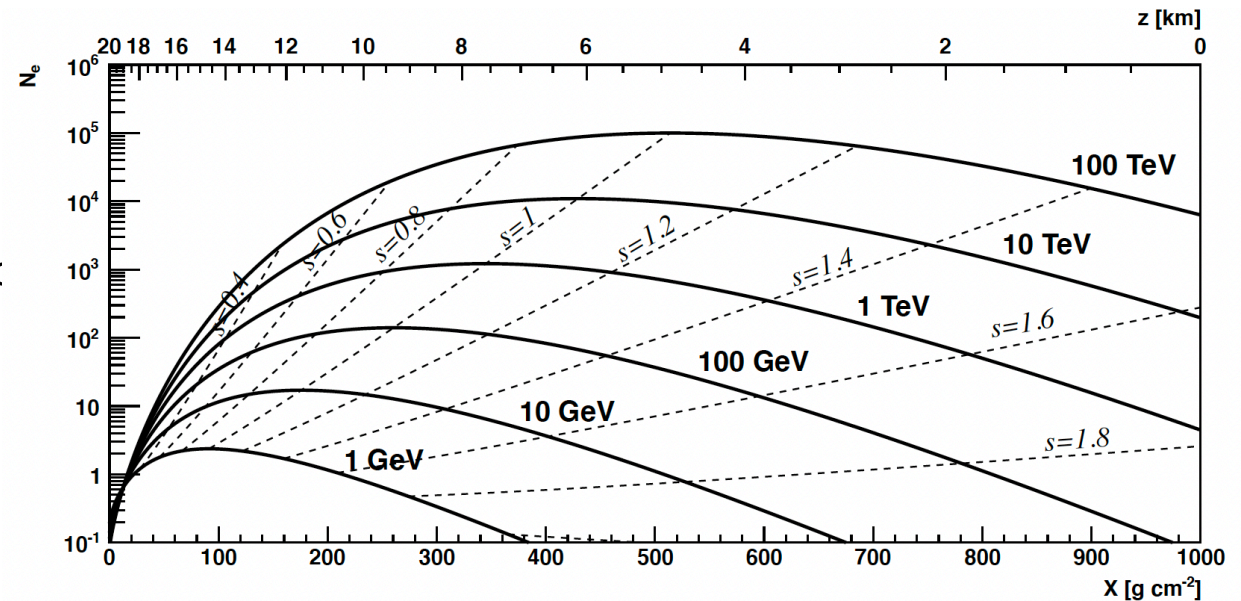
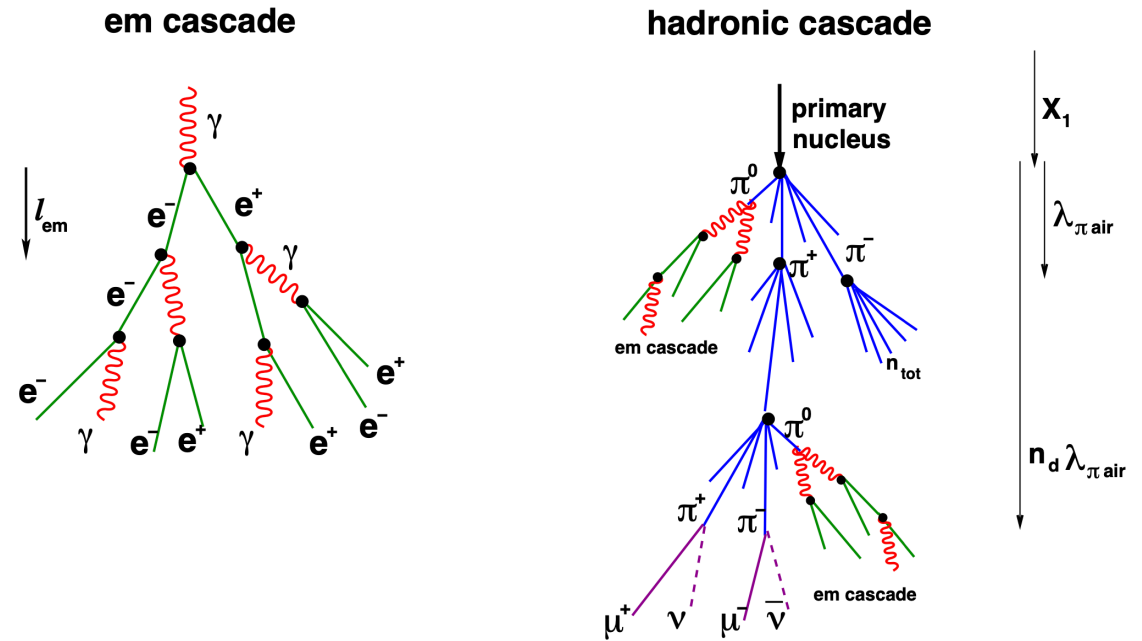
Shower maximum:  $N_{max} \propto \frac{E_0}{E_c}$  after  $n_{max}$

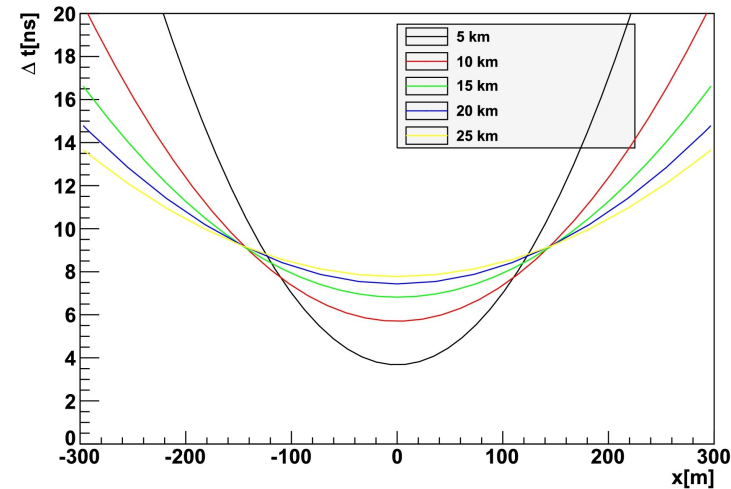
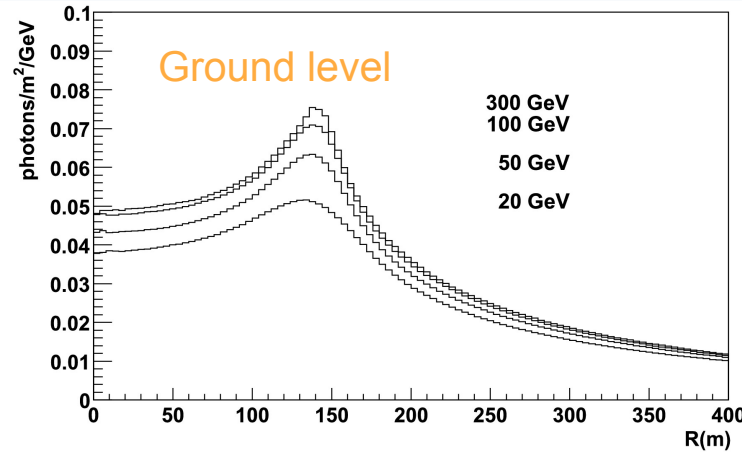
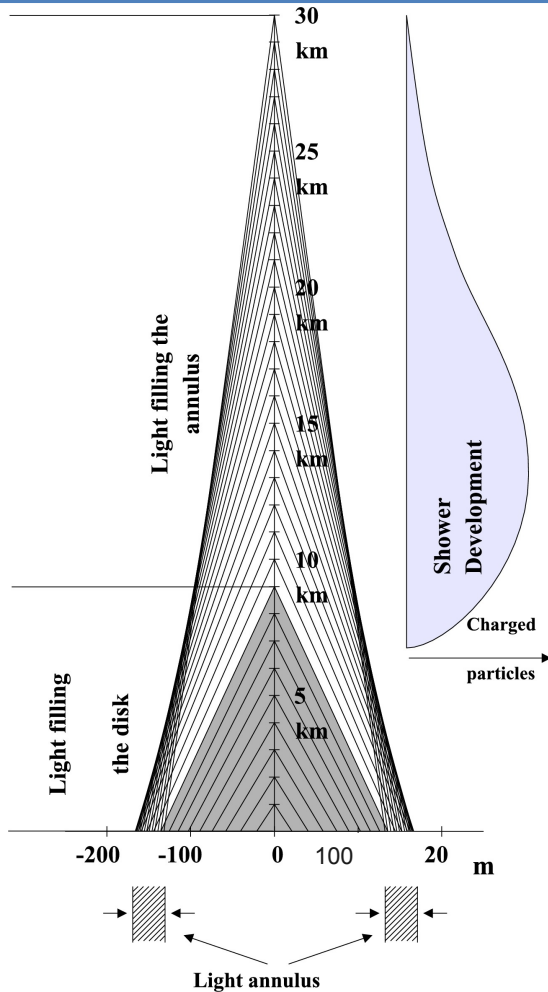
interaction lengths  $N_{max} = 2^{(n_{max})} \Rightarrow$

$$X_{max} \sim n_{max} \ell = X_0 \ln \left( \frac{E_0}{E_c} \right)$$

Cherenkov light is emitted by electrons ab

$$E_{th} = \frac{m_e c^2}{\sqrt{1 - 1/n^2}} \sim 40\text{MeV at 10 km in altitude in the atmosphere}$$





altitudes of emission

The charged particles in the shower travel faster than light in air, so close to the shower axis the photons emitted at low altitude reach the detector before those emitted at high altitude. At large impact distance of the photons emitted at low altitude have a longer geometrical trajectory (track of charged particle to emission point + photon track). On axis time is  $\sim 5$  ns.

1948 PMS Blackett (Nobel):  $\approx 0.01\%$  of the night light sky comes from Cherenkov light emitted by CRs and their secondaries as they traverse the atmosphere.

Experimental confirmation by C. Galbreith & J. Jelley, 1953

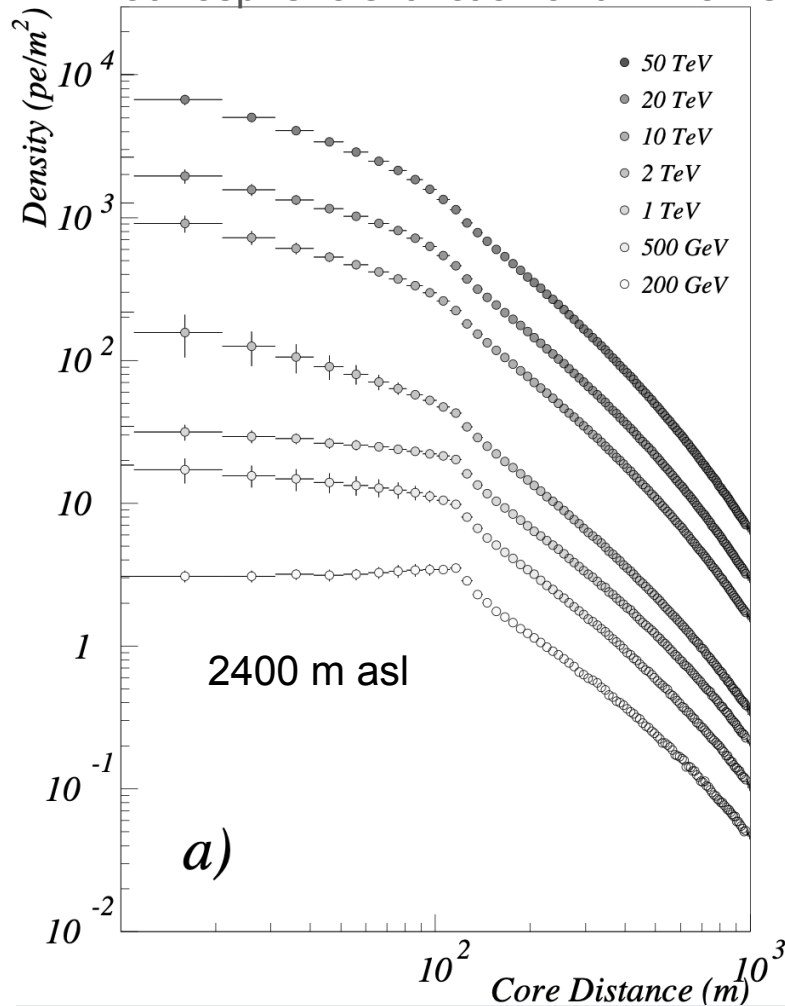
1989: Crab Nebula discovery by Whipple

$E_0$	$X_{\max}$ ( $\text{g cm}^{-2}$ )	Altitude (m)	$N_{\max}$
30 GeV	216	12000	50
1 TeV	345	8000	1200
1000 TeV	600	4400	$0,9 \times 10^6$
$10^{19}$ eV	936	1200	$7,4 \times 10^9$

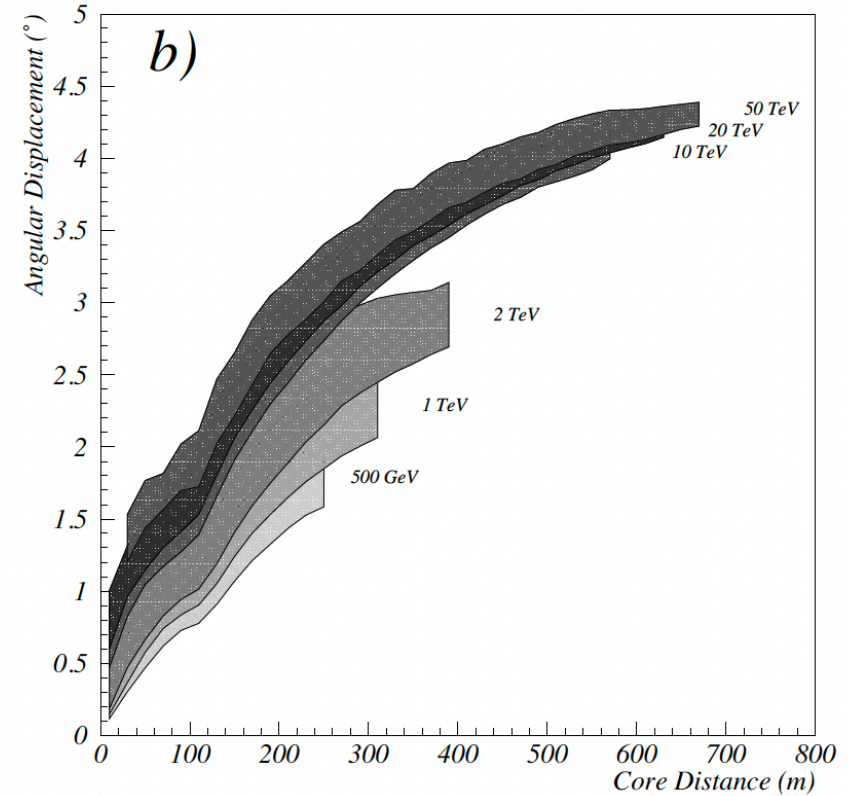
# Photoelectrons in the camera



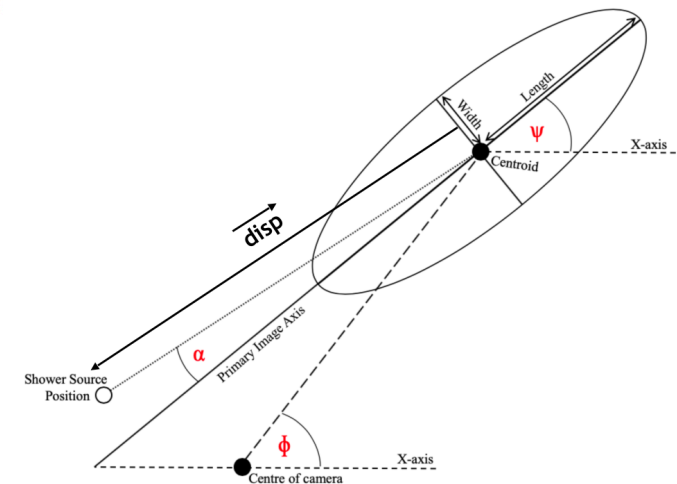
Photons after PDE of photosensor, atmospheric extinction and mirror reflectivity



Images from showers at larger core distances tend to have an average angle in the camera which is more displaced from the source position.

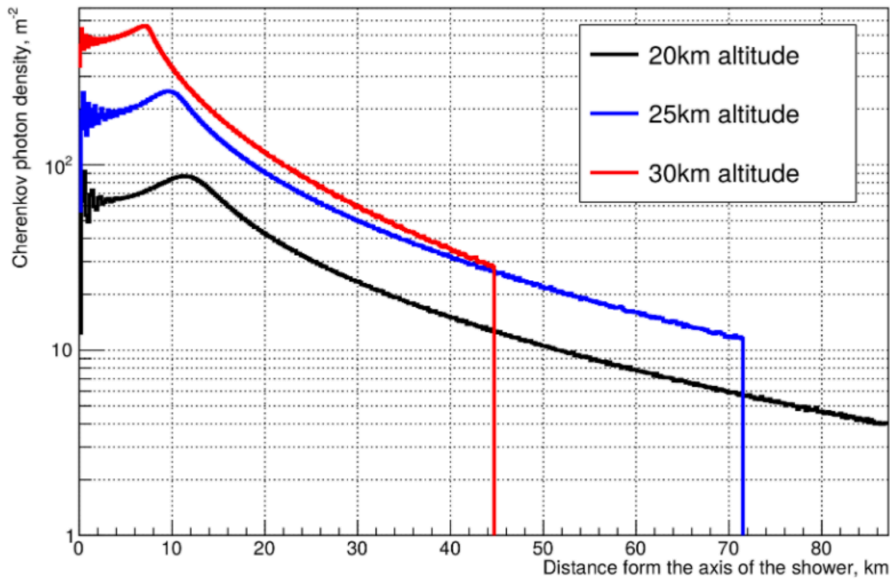


- Centroid: image center of gravity (first moments of light distribution in camera)
- Length and width of the ellipse (second moments)
- Size (total charge of photo-electrons in the image)
- $\phi$  angular distance between the centre of the camera and the image centre of gravity
- $\Psi$  azimuthal angle of the image main axis (second moments)
- $\alpha$  orientation angle of source from image axis

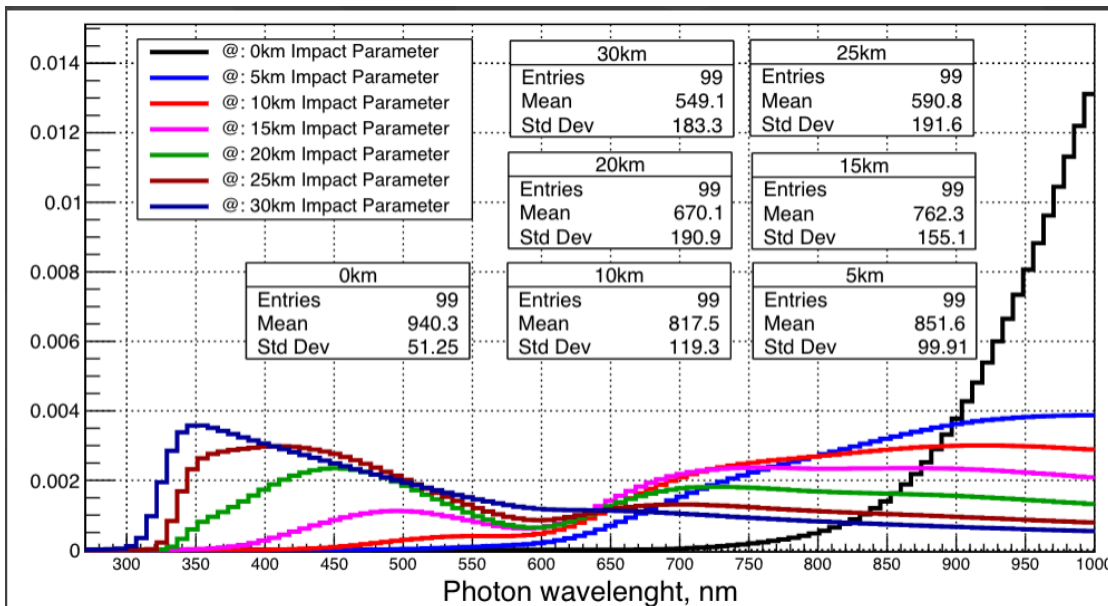
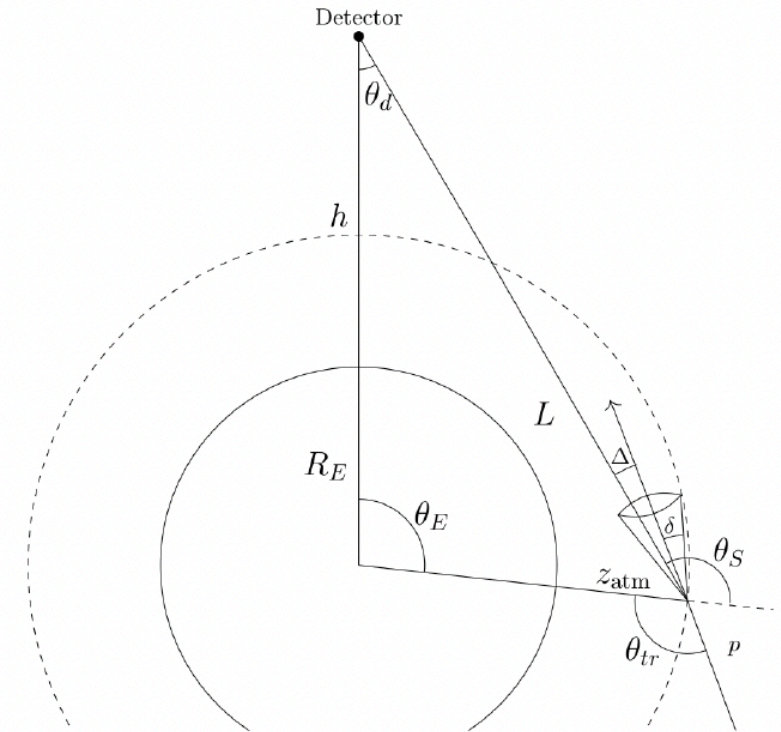


# Cherenkov from space

100 PeV UHECR showers in the limb as seen from different altitudes seen from 535 km orbit



Simulation from Cummings, Aloisio, Eser, Krizmanic, 2021

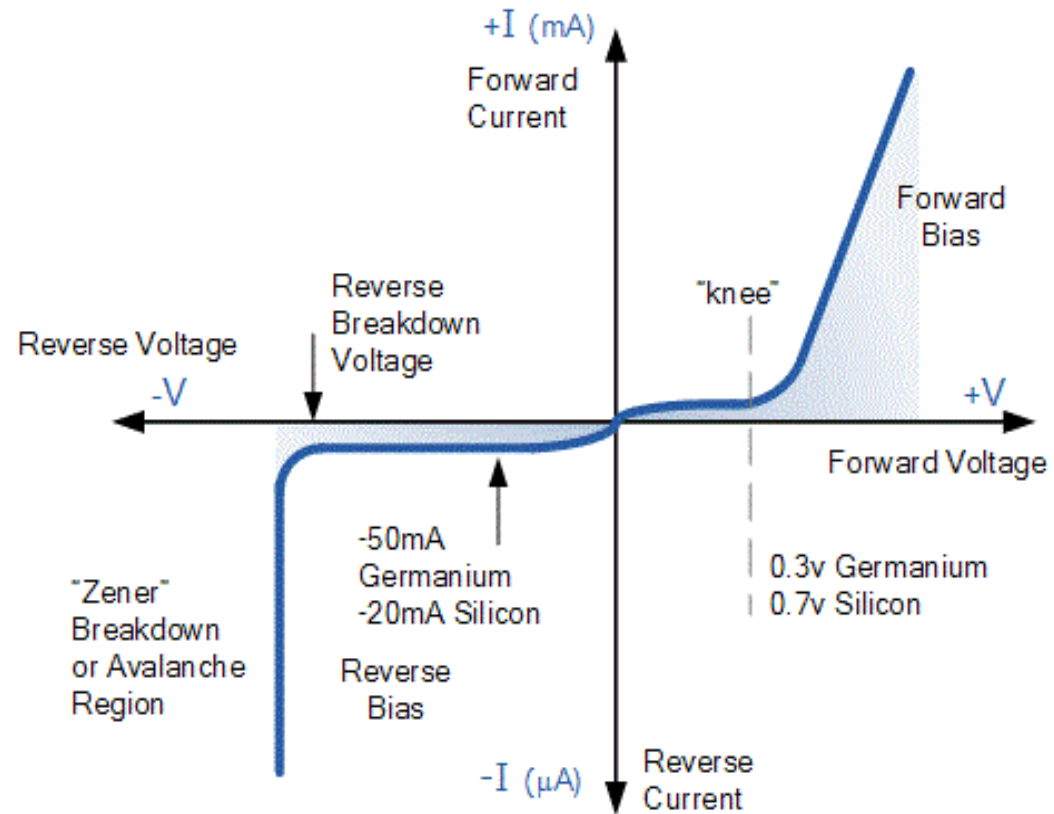
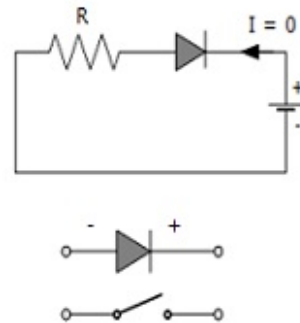
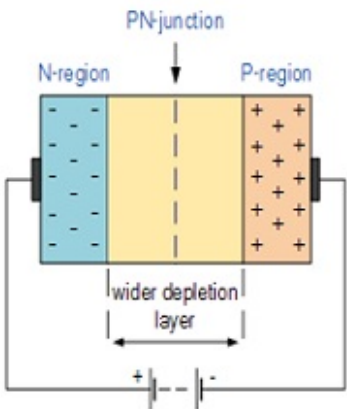
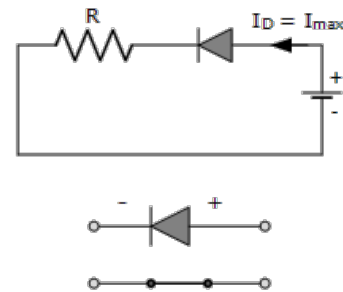
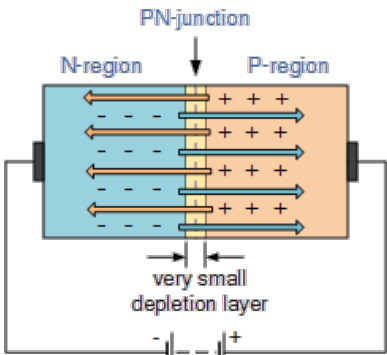
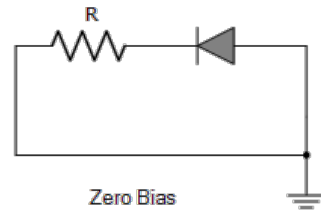
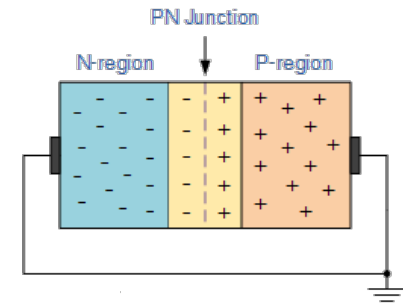


Cherenkov spectrum for UHECRs at different altitudes seen from 535 km

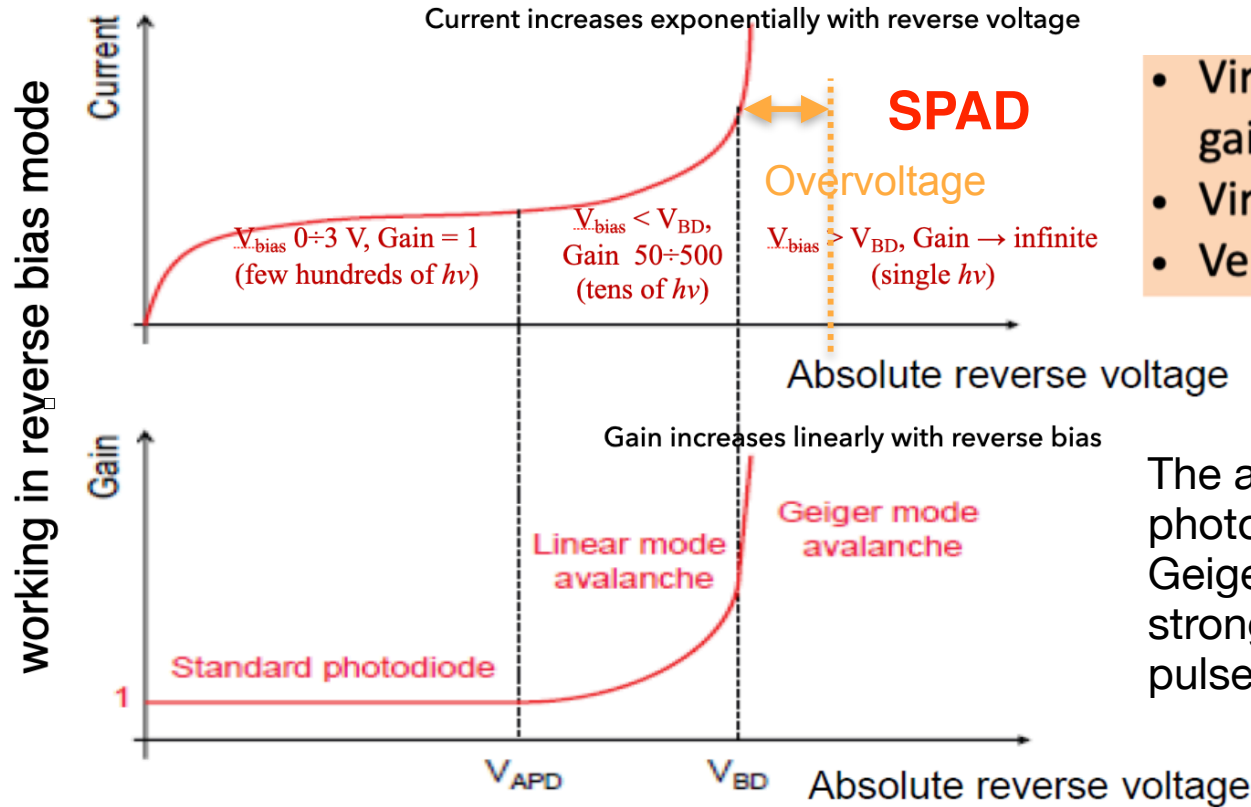
# Diode : a pn junction



$$I = I_0 \left( e^{-eV/kT} - 1 \right)$$

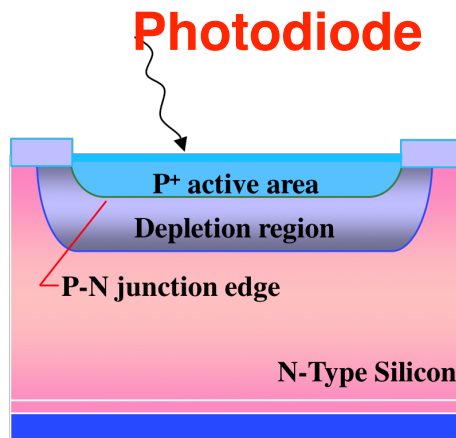


Photons create e-h pairs in the depleted layer which can be used to detect light

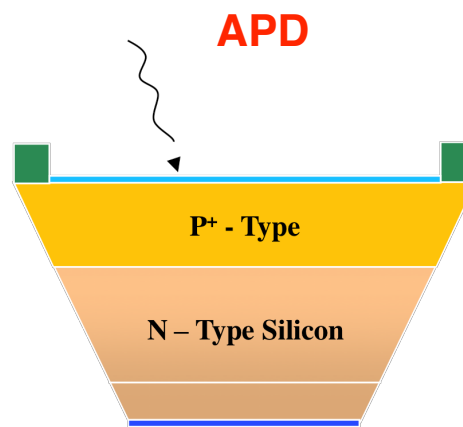


- Virtually infinite optical gain
- Virtually zero noise
- Very fast

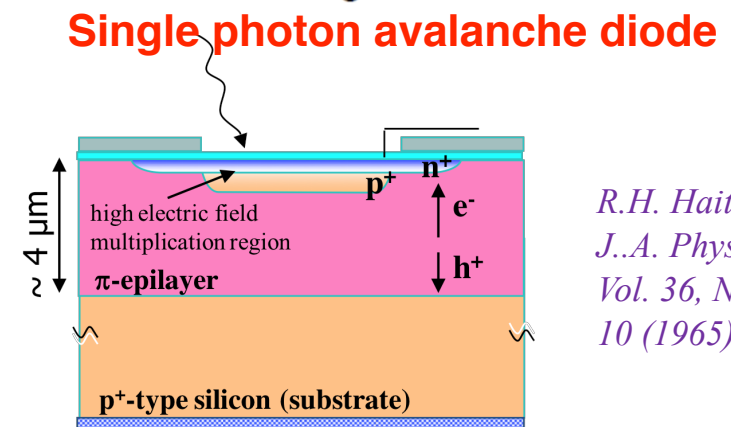
The absorption of single photon in photodiodes in Geiger mode can initiate a strong avalanche current pulse



p-n junction,  
reversed  $V_{bias} = 0-3 \text{ V}$



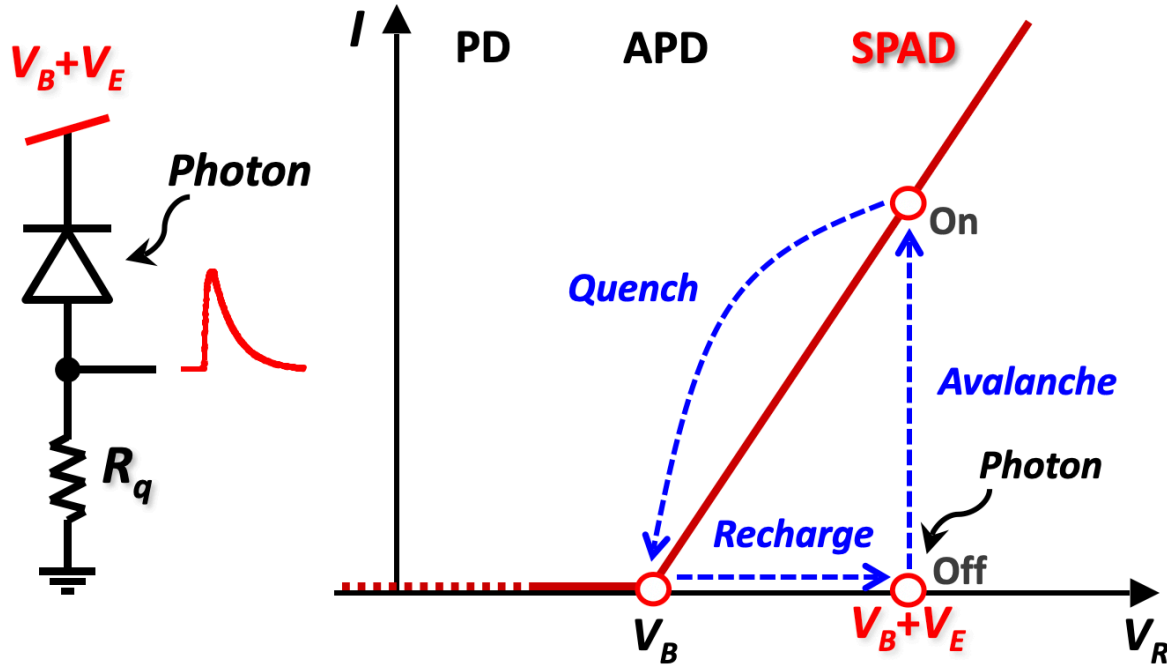
p-n junction,  
reversed  $V_{bias} < V_{BD}$



p-n junction,  
reversed  $V_{bias} > V_{BD}$

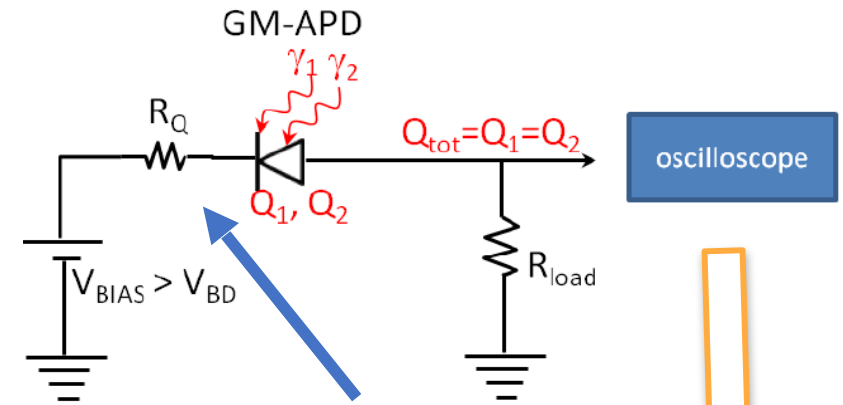
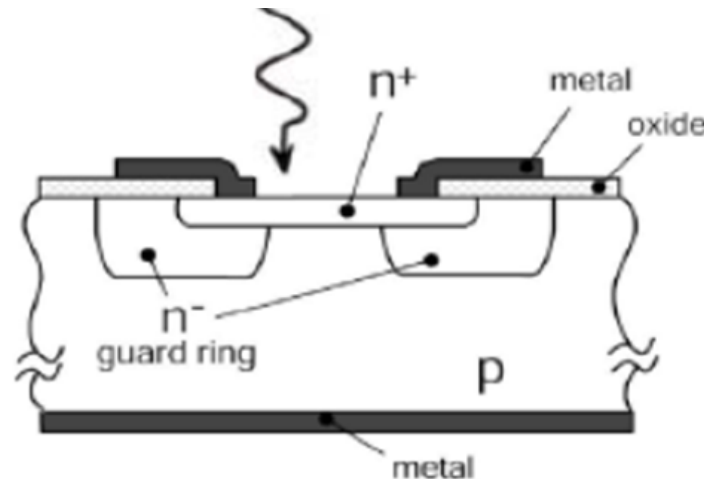
*R.H. Haitz,  
J..A. Phys.,  
Vol. 36, No.  
10 (1965)*

- The avalanche can be passively quenched

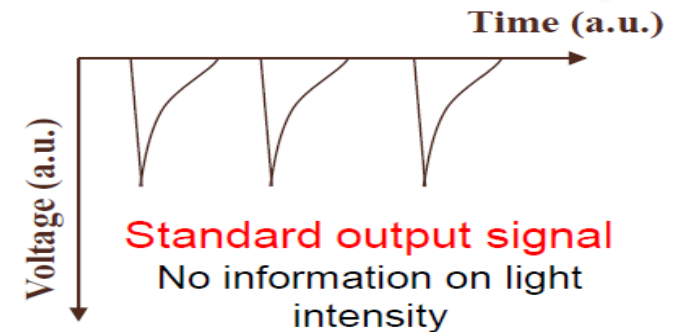


© 2018 Edoardo Charbon

11



to quench  
avalanche

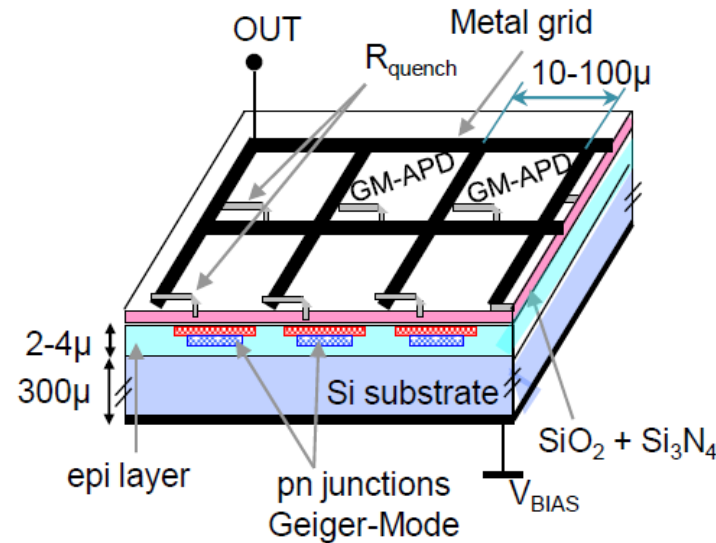


Digital device

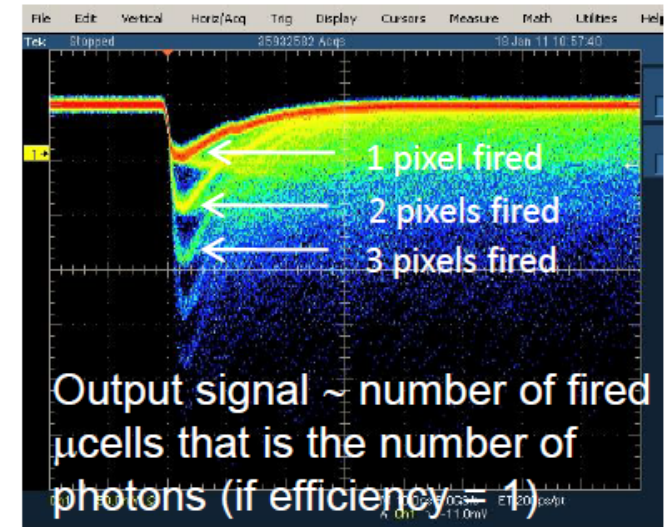
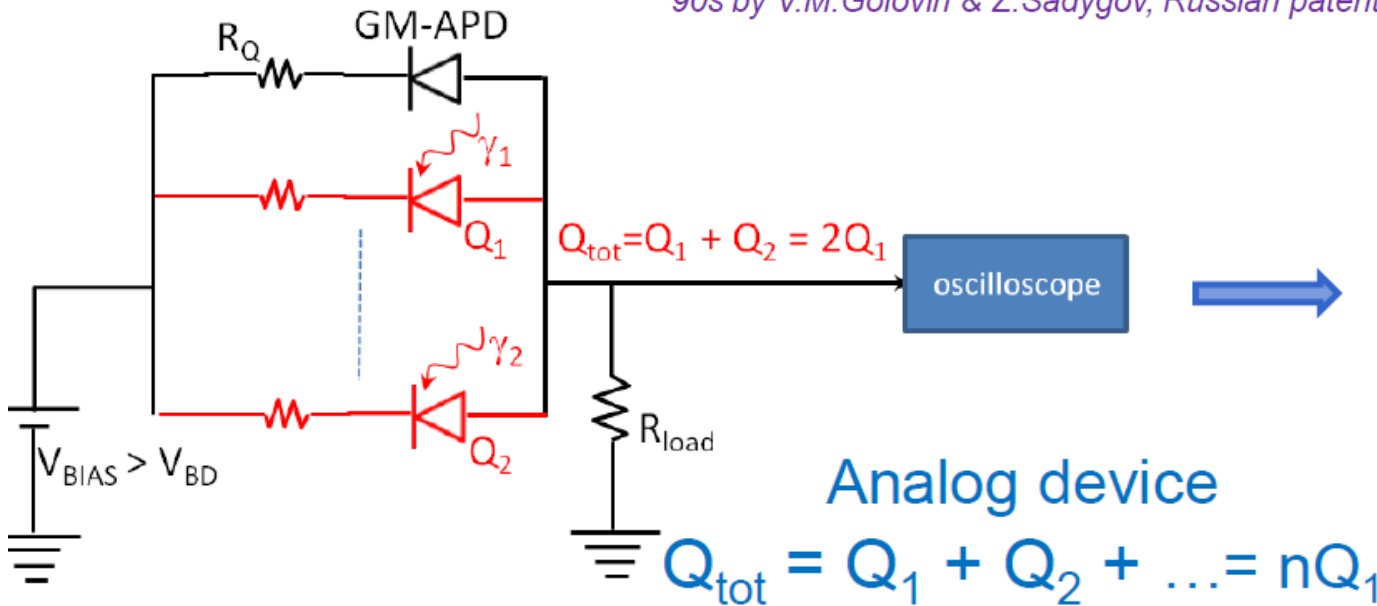
$$Q = Q_1 = Q_2 = \dots = Q_n$$



- Parallel array of SPADs or  $\mu$ cells on the same substrate and each SPAD in series with  $R_q$



'90s by V.M.Golovin & Z.Sadygov, Russian patents



# The quanta information from G-APDs

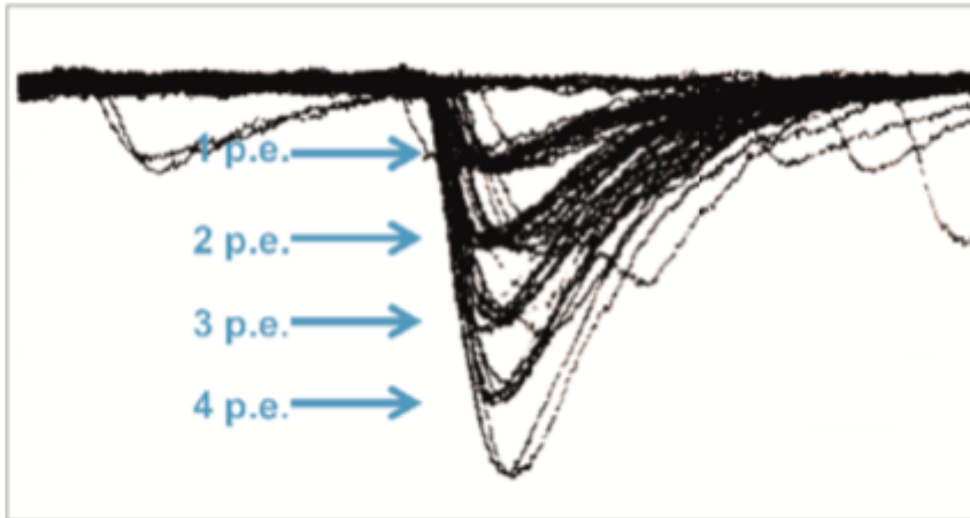


Figure 6, Oscilloscope shot showing the discrete nature of the SiPM output when illuminated by brief pulses of low-level light.

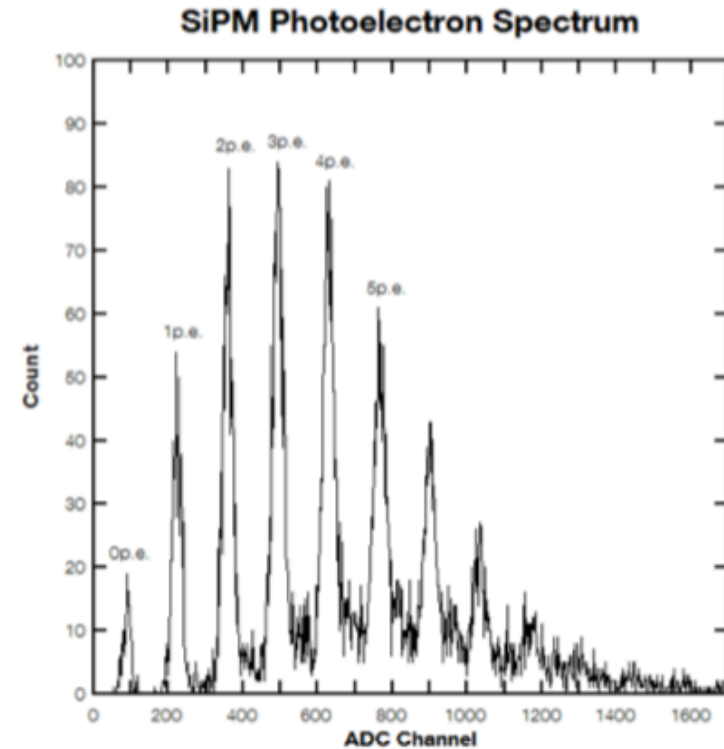


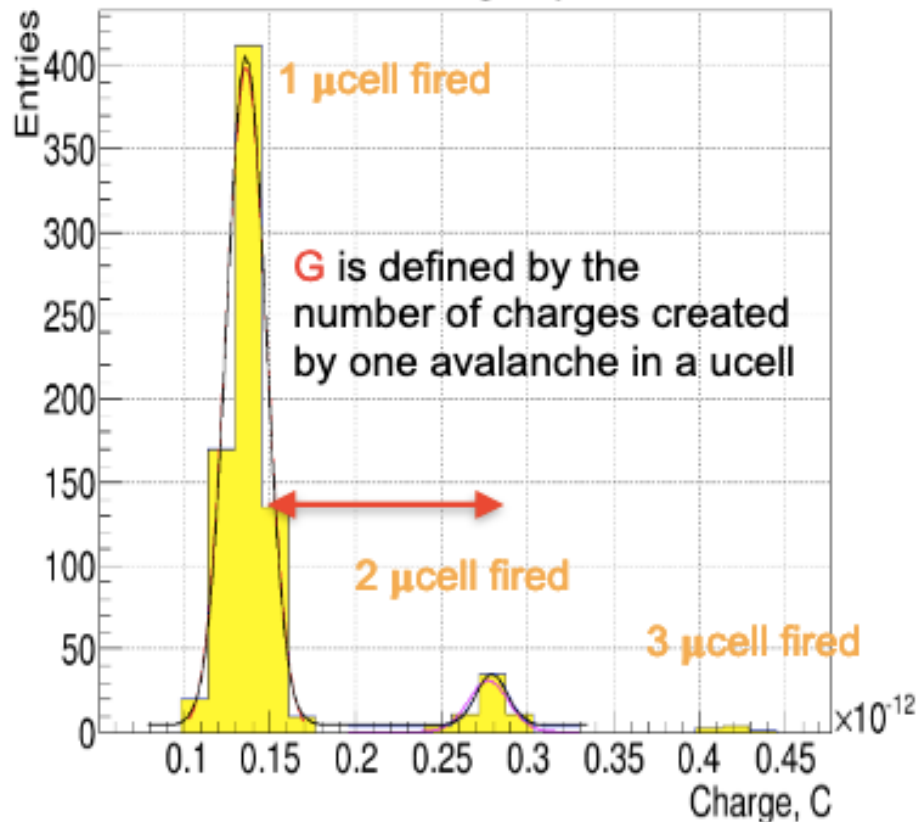
Figure 7, Photoelectron spectrum of the SiPM, achieved using brief, low-level light pulses, such as those from Fig. 6.

The sum of the photocurrents from each  $\mu$ cell combines to output the magnitude of the impinging photon flux. In practice, G is measured from integration of pulse - baseline.

$$G = \frac{Q}{e} = \frac{1}{G_{Amp} \cdot e} \cdot \frac{1}{R} \int (V(t) - BL) dt,$$

Amplifier input impedance

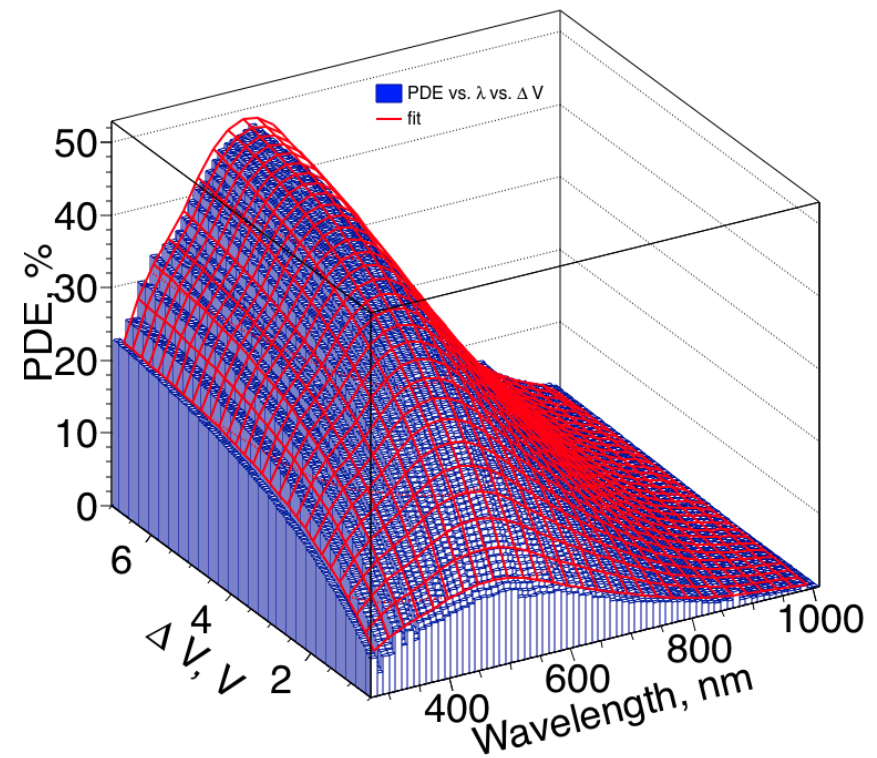
Charge spectrum



QE – probability to create an e/h pair

$P_{Geiger}$  – probability that e/h triggers an avalanche

FF – ratio between active and total areas

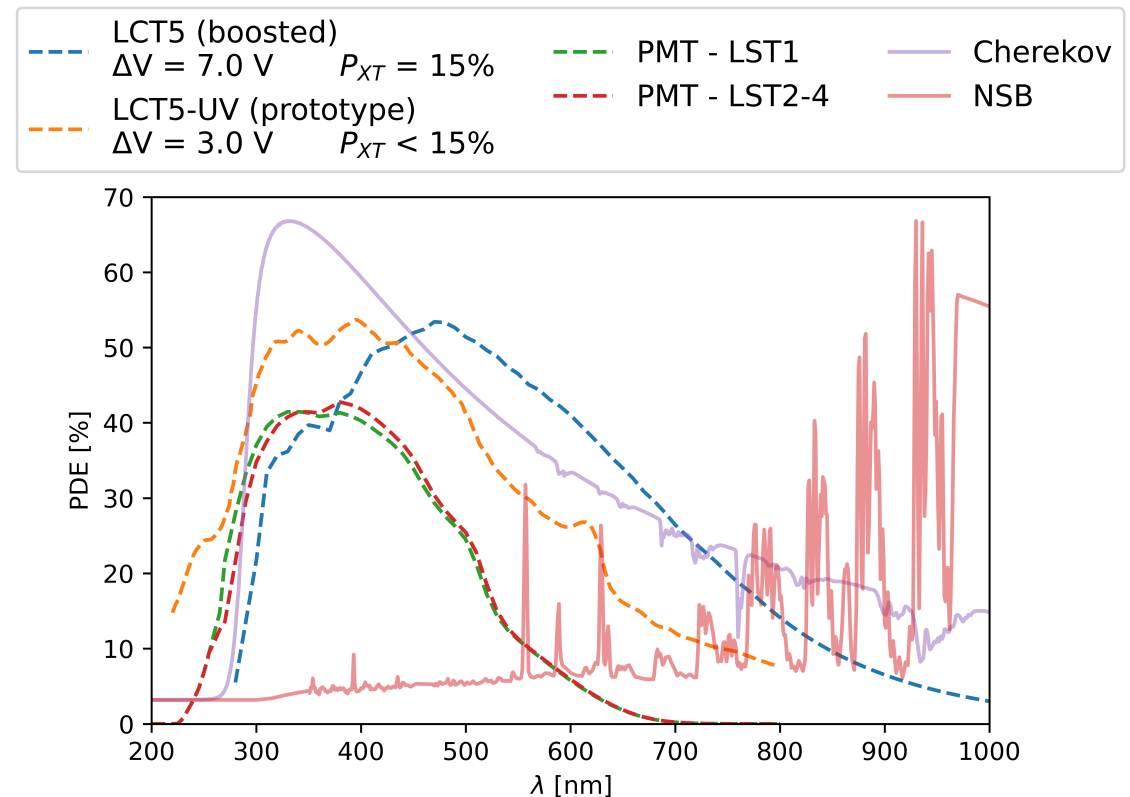
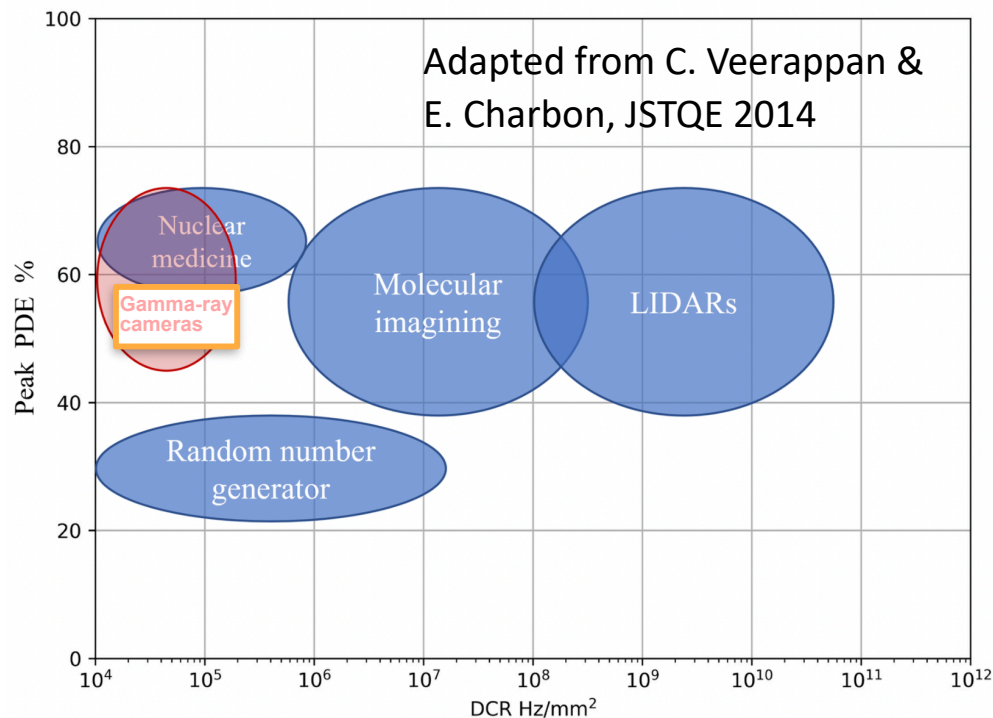


## Advantages:

- robustness to light (~30% more observation time)
- Mass producibility, low power, cost
- Uniformity, negligible ageing

## Challenges:

- high sensitivity in night sky background region  $> 500$  nm
- PDE  $> 10\%$  than PMTs but max at too high wavelength for Cherenkov spectrum; need to work at high over-voltage with consequent Xtalk increase and also Voltage drop effect
- Filters on entrance window (e.g. in borofloat) improve performance at high energy, at low energy it cuts more Cherenkov signal than PMMA window (on which coating cannot be applied)

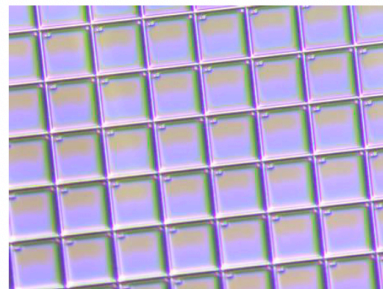
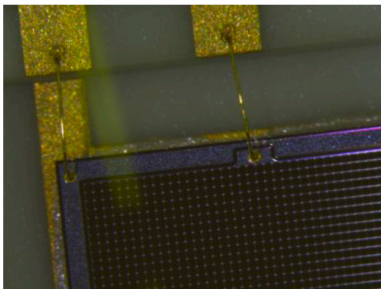


# G-APD developments

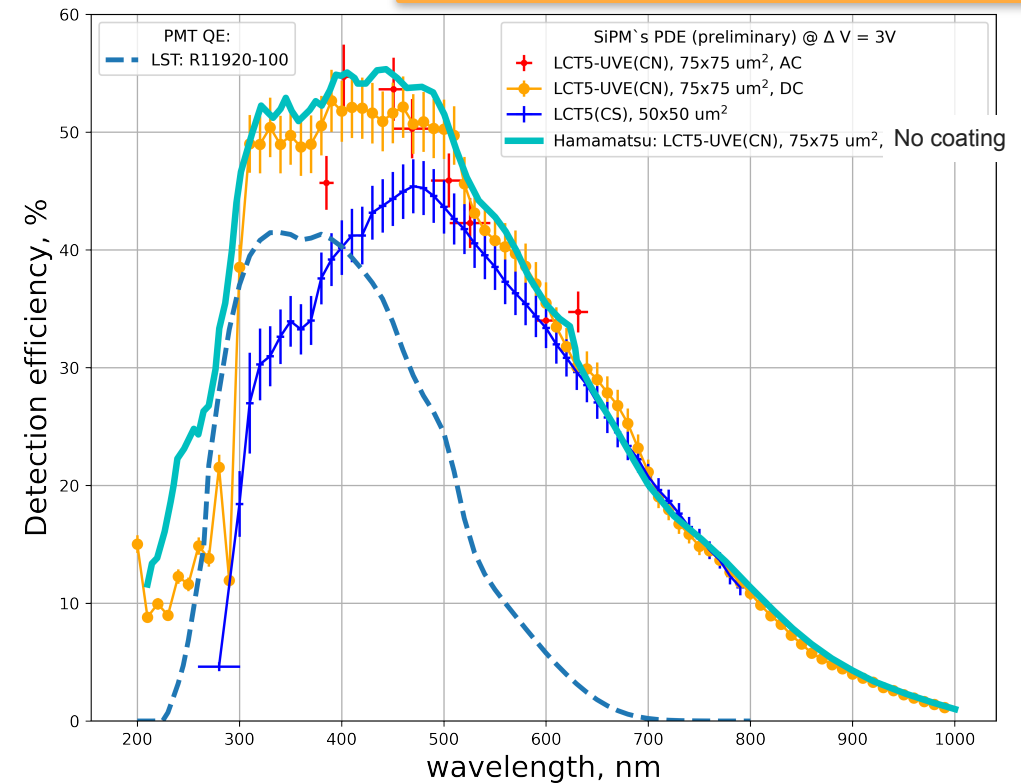


- Based on LCT5 (S13360) technology:
  - Improved UV sensitivity;
  - Reduced IR sensitivity;
- Size of  $3 \times 3 \text{ mm}^2$  ;
- Pixel size  $75 \times 75 \text{ } \mu\text{m}^2$  ;
- Without Coating

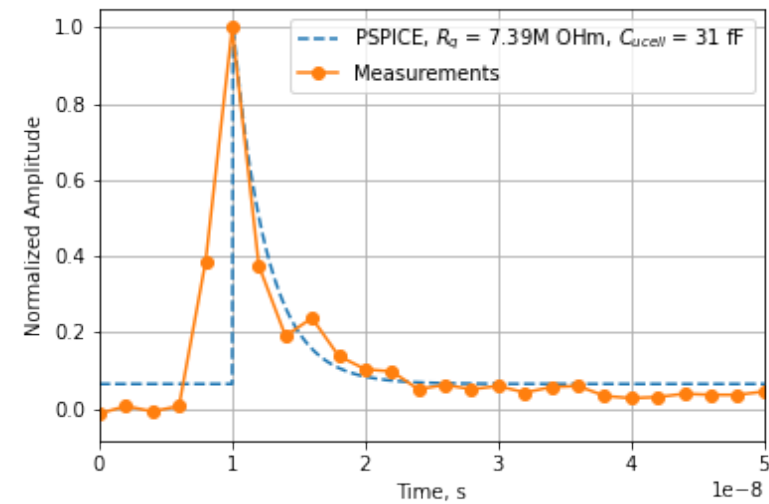
$$V_{BD} = 52.783 \text{ V}$$



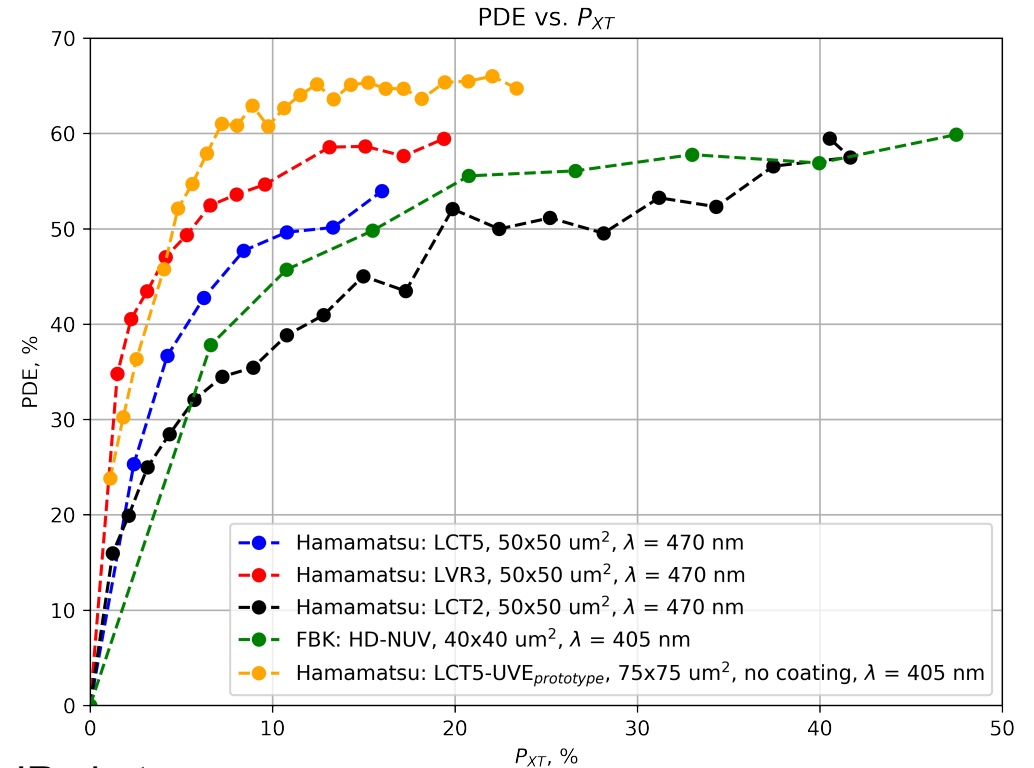
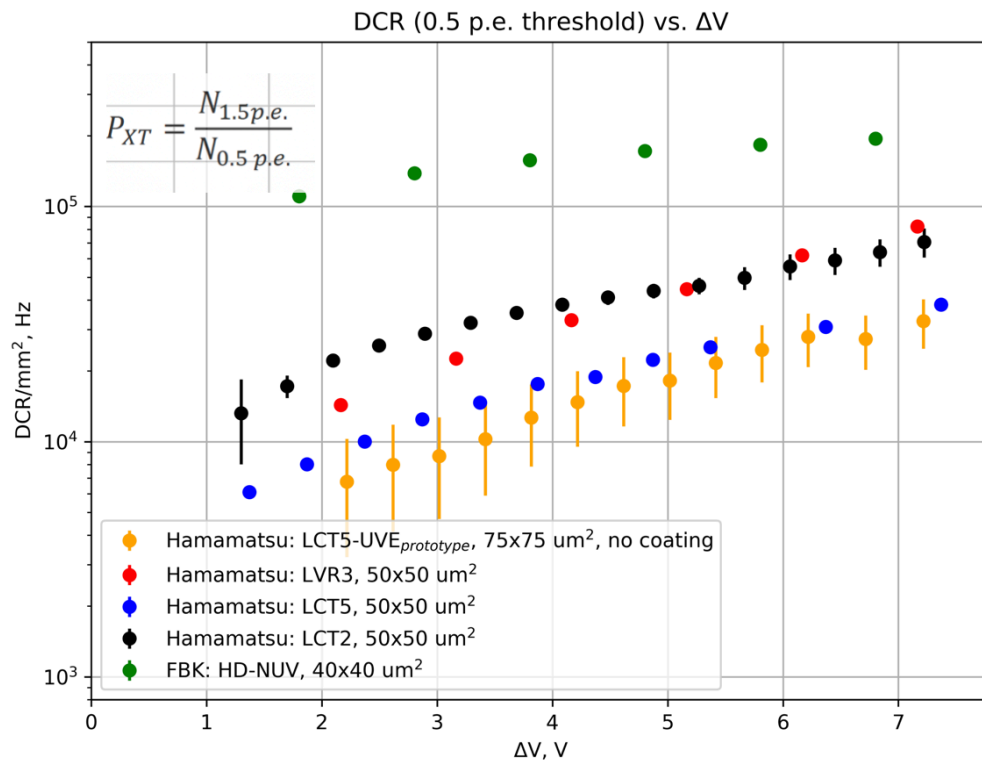
## LCT5-UV Prototype - preliminary



- Preliminary results from a new sensor by Hamamatsu:
  - ◆ Similar performance to former devices in term of noise
  - ◆ Large improvement in sensitivity in the UV compared to standard SiPM and PMTs
  - ◆ Remarkably short pulse ( $\sim 3 \text{ ns}$  FWHM) without specific shaping
- Possibly a coating to reduce IR contribution?

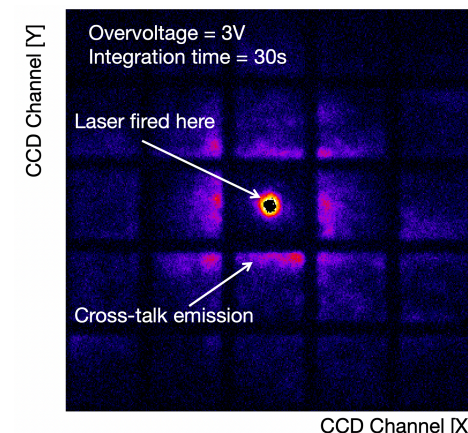
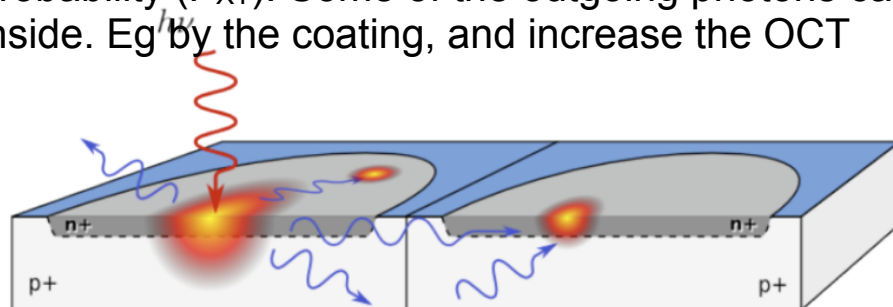


# Uncorrelated and Correlated noise



OXT : the avalanche process in a  $\mu$ cell emits secondary IR photons that are then detected by the surrounding  $\mu$ cells with a certain probability ( $P_{XT}$ ). Some of the outgoing photons can be reflected inside. Eg by the coating, and increase the OCT

D. Strom & R. Mirzoyan, PD18, Japan



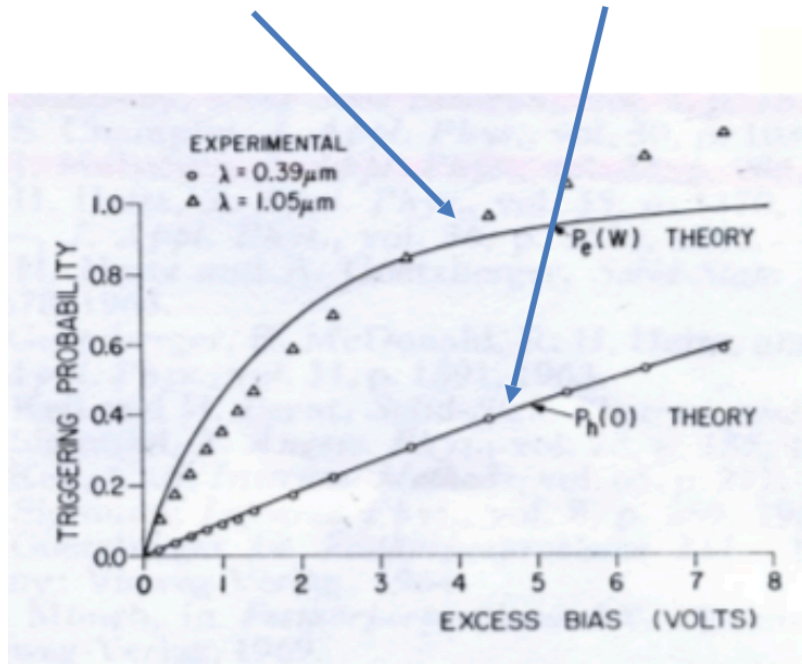
# Sensitivity range



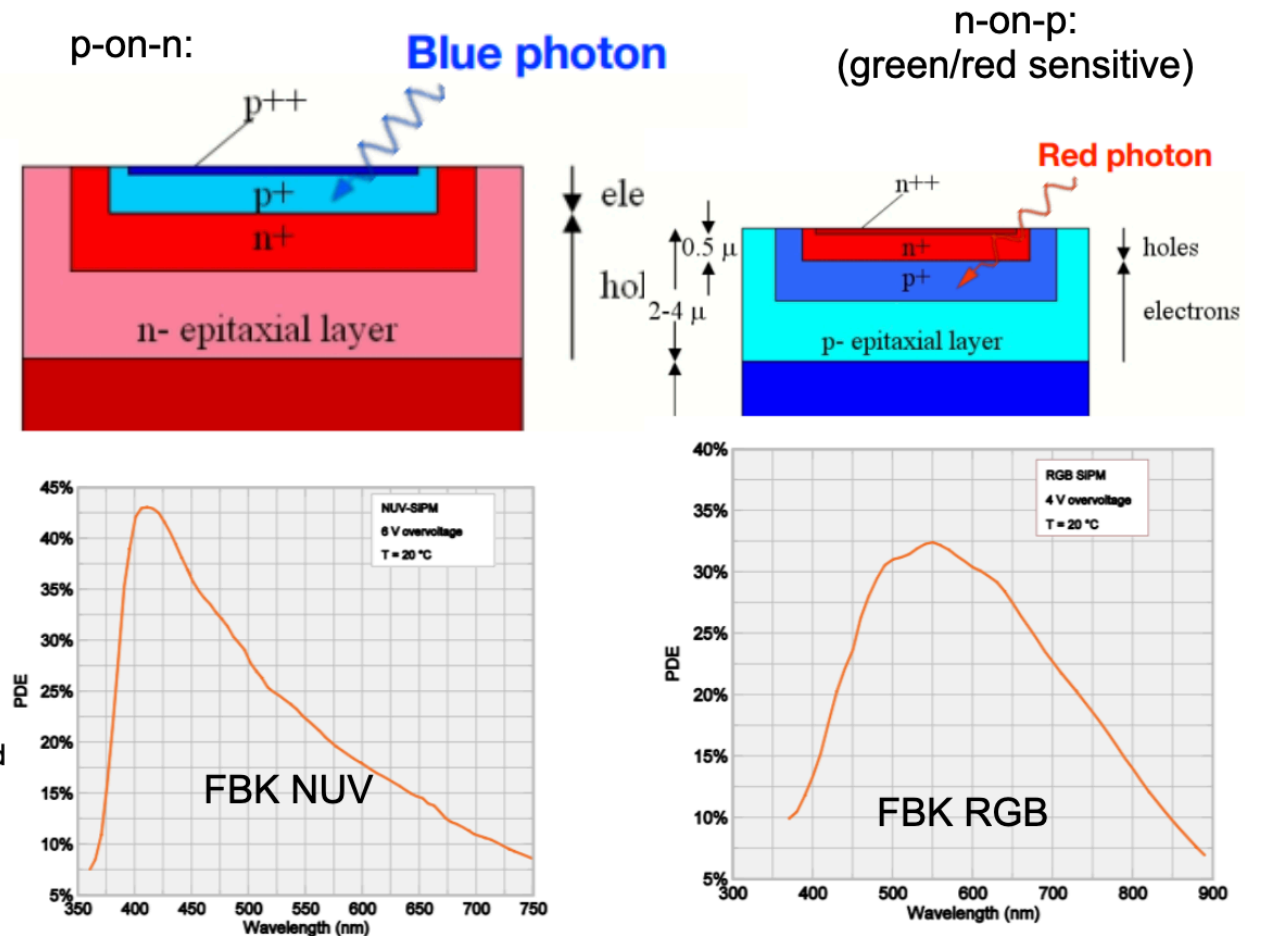
The PDE is given by :  $PDE(\lambda, \Delta V) = QE \times CE = QE(\lambda) \times P_G(\Delta V) \times FF$

$P_G(\text{electron}) \gg P_G(\text{hole})$  :

Two types of junction:



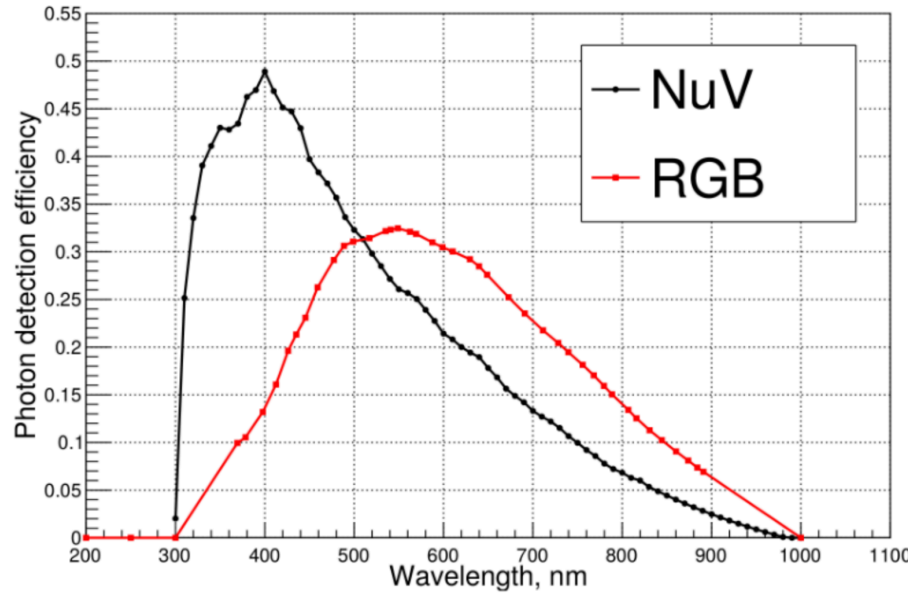
This plot was measured for the n-on-p junction where we need red light to penetrate to p+ layer where electrons are produced. The electron avalanche trigger probability has exponential behaviour



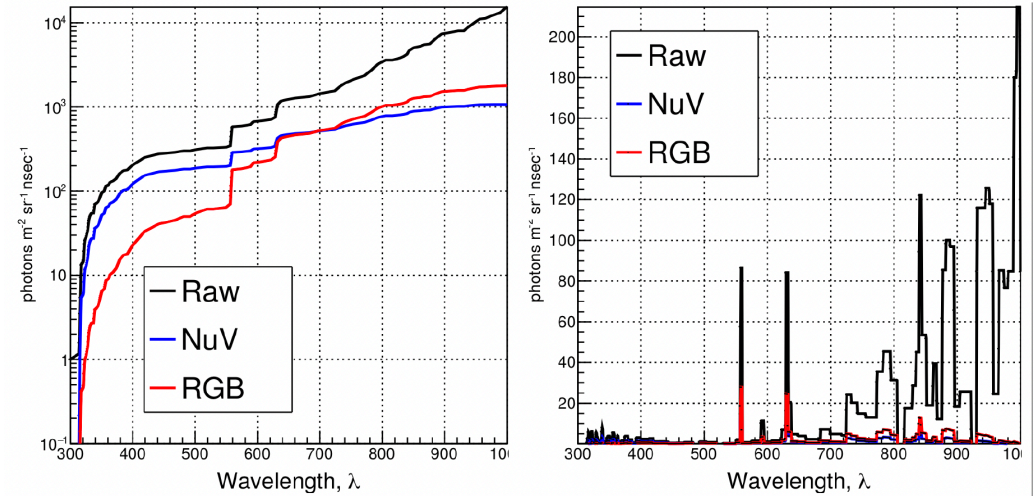
# What detectors for Cherenkov from space?



SiPM PDE vs wavelength



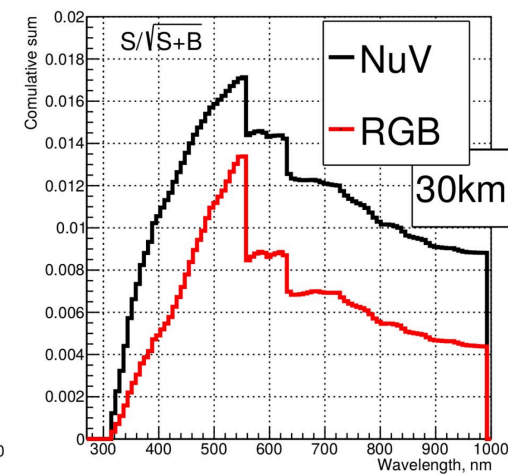
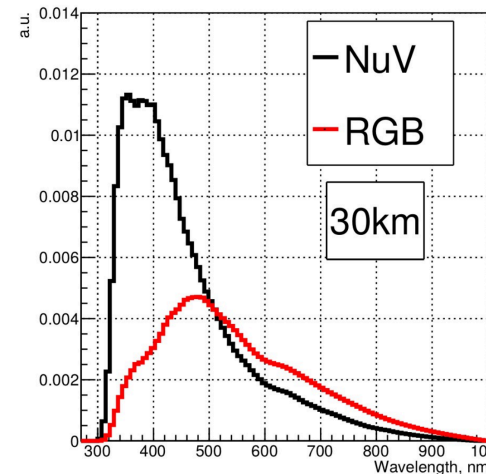
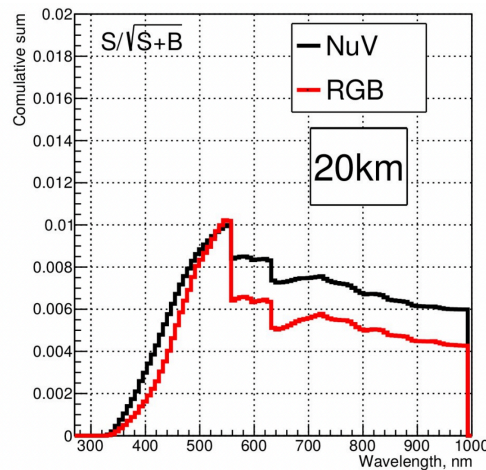
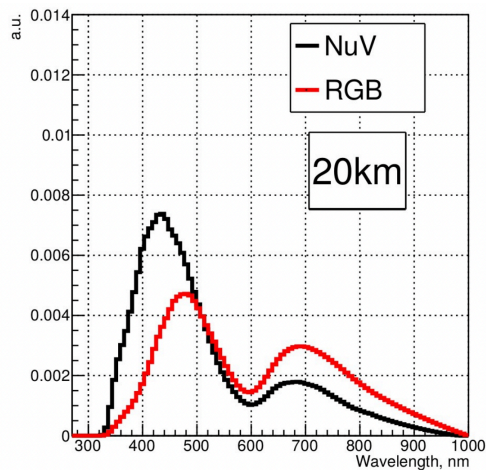
Convolved Night glow with PDE in log and Lin scale (arxiv:2008.04984):



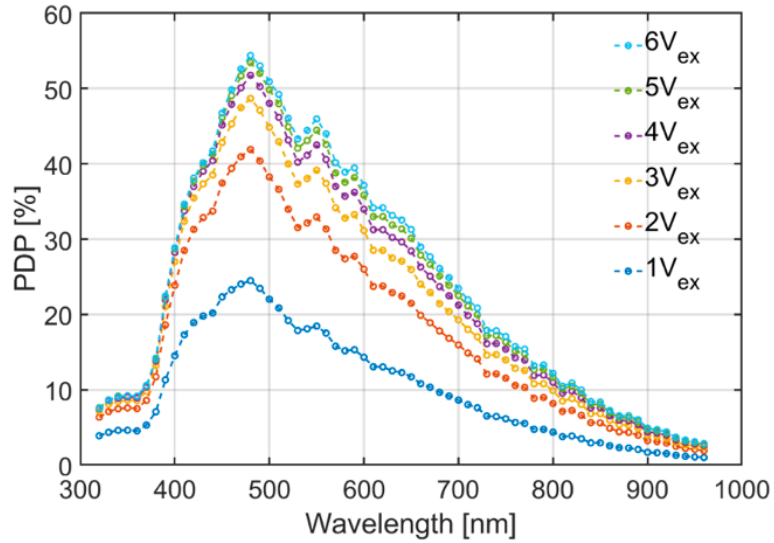
L. Burmistrov

3

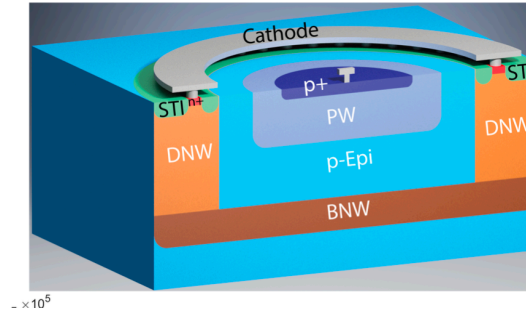
## Convolved Cherenkov signal with PDE





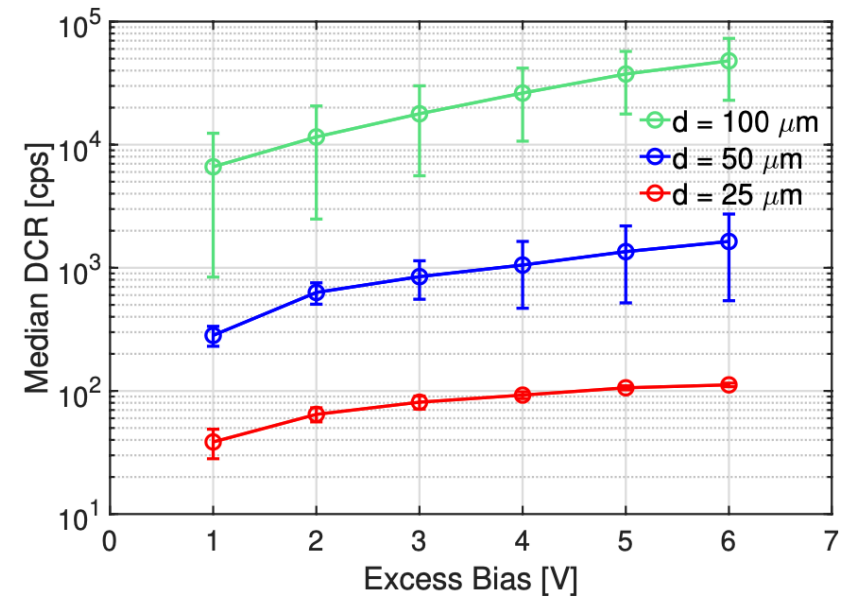
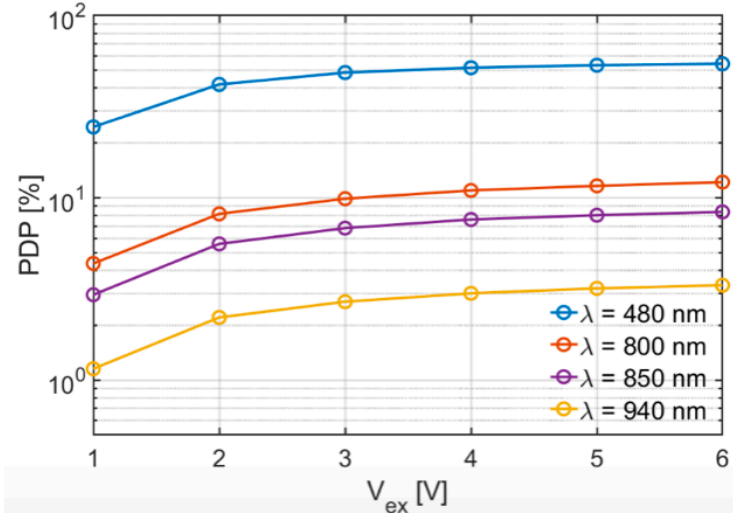


180 nm CMOS technology



State-of-the-art CMOS SPADs:  
0.1~10Hz/ $\mu\text{m}^2$

Analog SiPM have 2-3 orders of magnitude lower DCR rate



PhotoDetection Probability does not account for Fill Factor. Solution with micro lenses on each SPAD allows to keep PDE high.

Fig. 5. DCR median value measured at several excess bias voltages for the different SPAD sizes. The results are obtained measuring 15 devices for each size.

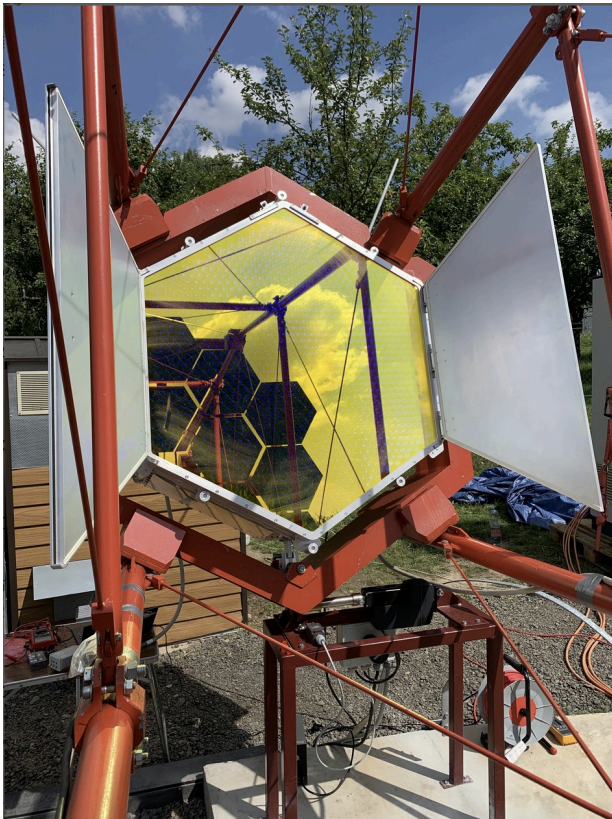
# Application : SST-1M camera



UNIVERSITÉ  
DE GENÈVE

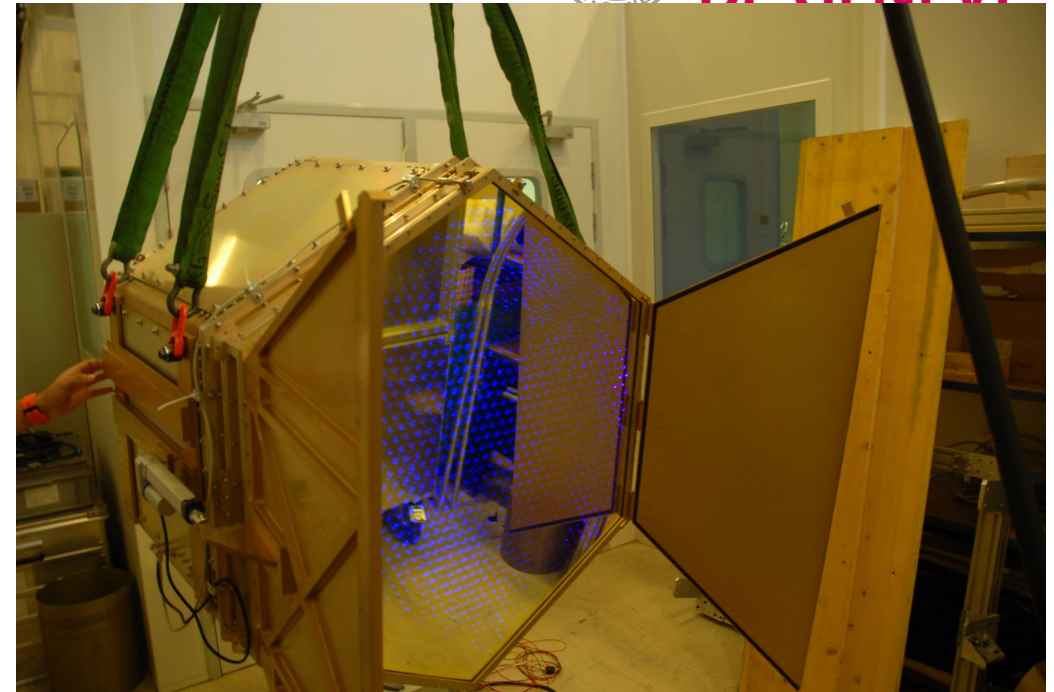


Initially developed for CTA as  
prototypes of SSTs  
Was reviewed and satisfied all  
requirements  
Now two SST-1Ms are installed at  
Ondrejov Observatory (CZ)  
for stereo tests and science  
commissioning



University College Dublin  
Ireland's Global University





**Dish = 4 m**

**FoV = 9°**

**f/D = 1.4**

Davies-Cotton design

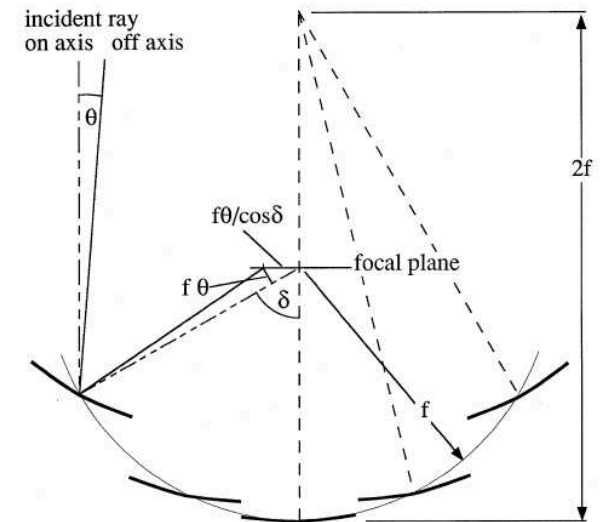
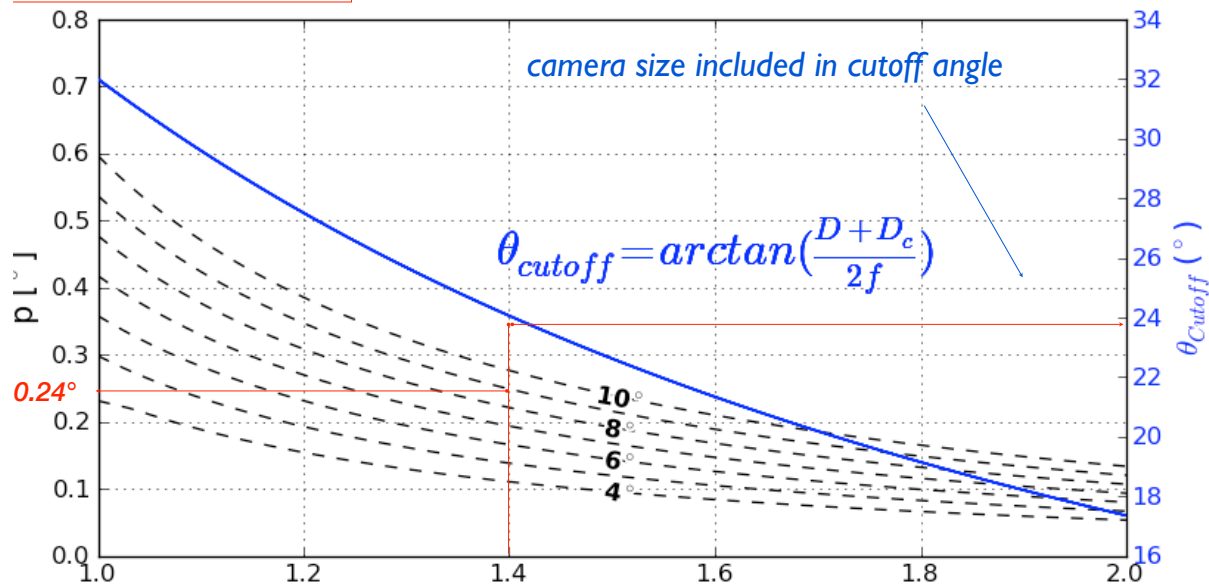
Pixel size =  $4 \cdot \min(\sigma_x, \sigma_y) = 0.24^\circ$

Camera size ( $D_c$ ) = 88 cm

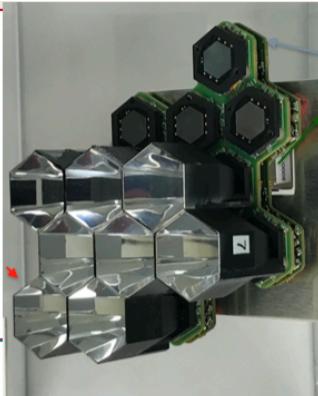
Pixel size (linear) = 2.32 cm

$n_p = 1296$  pixels

Watch us on Youtube:  
Video 1 (HD) Video 2



- Hollow light guides:**
- Cut-off at 24°
  - 2.32 cm linear size
  - Compression factor of ~6
  - dichroic coating



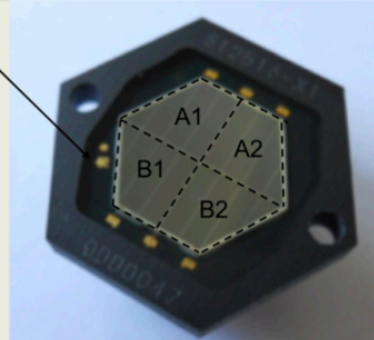
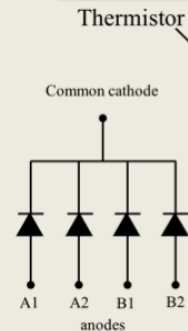
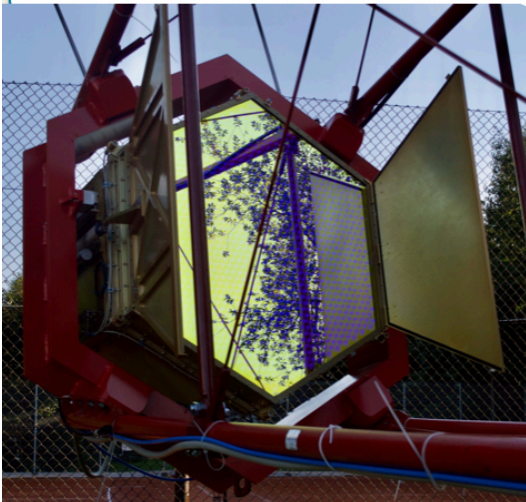
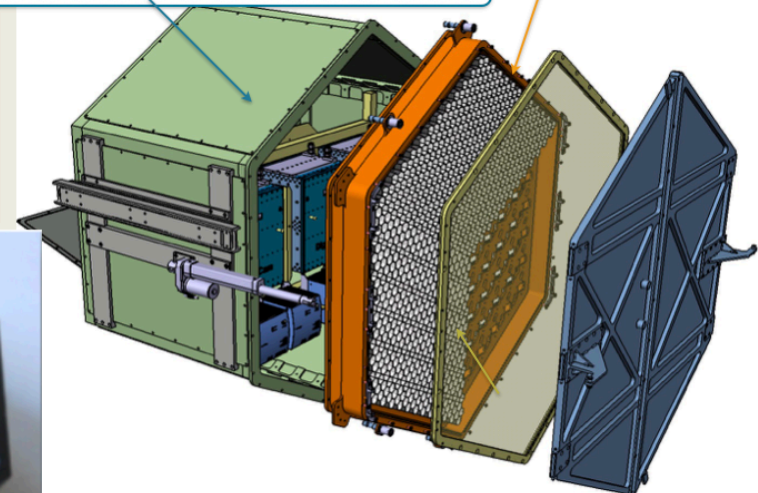
- Slow control board:**
- 108/camera
  - Temperature compensation loop Hz
  - HV generation

- 12 bits FADC @ 250 MS/s
- Fully digital trigger, reconfigurable and signal preprocessing
- Serial architecture based on multi-Gigabit links (both trigger and ADC data)
- Power consumption 1200 W

- Photo detection plane:**
- 1296 pixels
  - 0.24° angular size
  - Power consumption 500 W
  - Analogue signals over CAT5/RJ45

- Preamplifier board:**
- 108 /camera
  - discrete components
  - Trans-impedance topology
  - DC coupling

- Hamamatsu LCT2 50  $\mu\text{m}$
- 4 anodes per pixel with one common cathode
- NTC temperature sensor



1 cm<sup>2</sup> sensitive area  
 $V_{over} = 2.8 \text{ V} \Rightarrow C_{\mu\text{cell}} \sim 85 \text{ nF}$

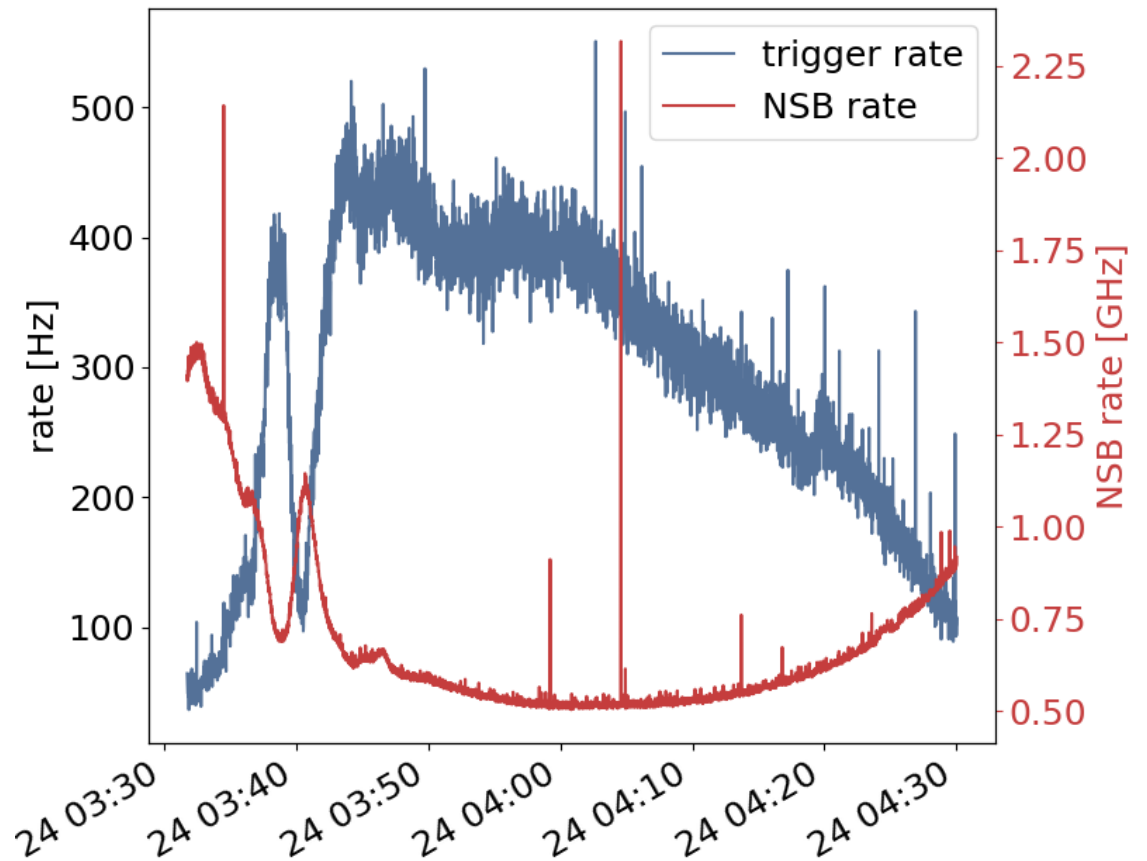
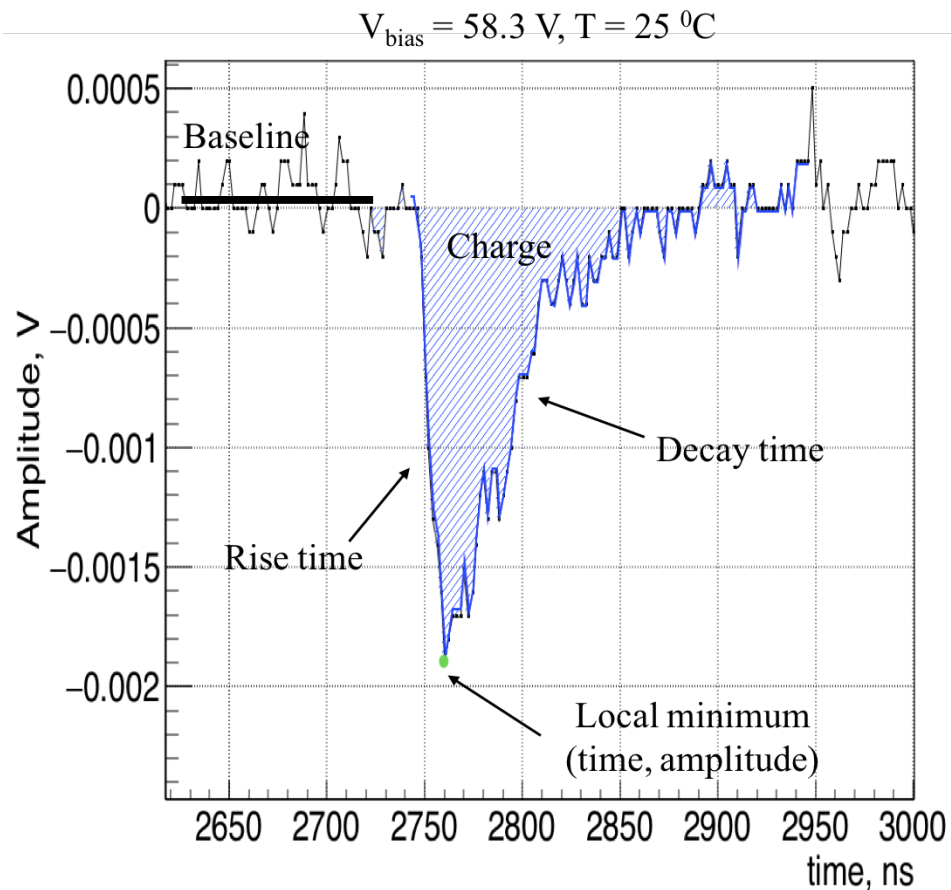
- Entrance window:**
- 3.3 mm Borofloat
  - Cut-off filter at 540 nm for NSB rejection

A DC coupled camera is NSB monitor!

The Digicam can measure the BL before each pulse.

Useful for correcting for changes of SIPM parameters

Rate of NSB in Krakow (including clouds and airplanes...)



# Voltage drop

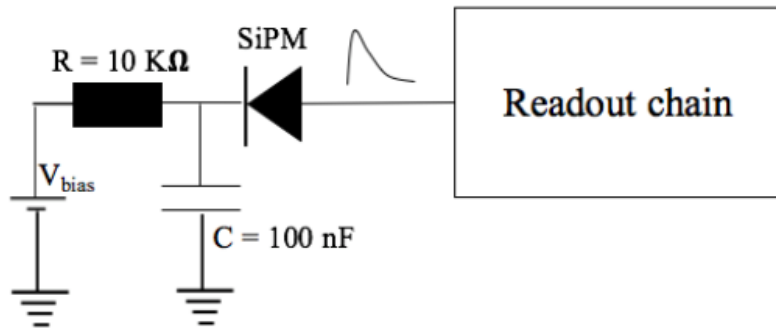
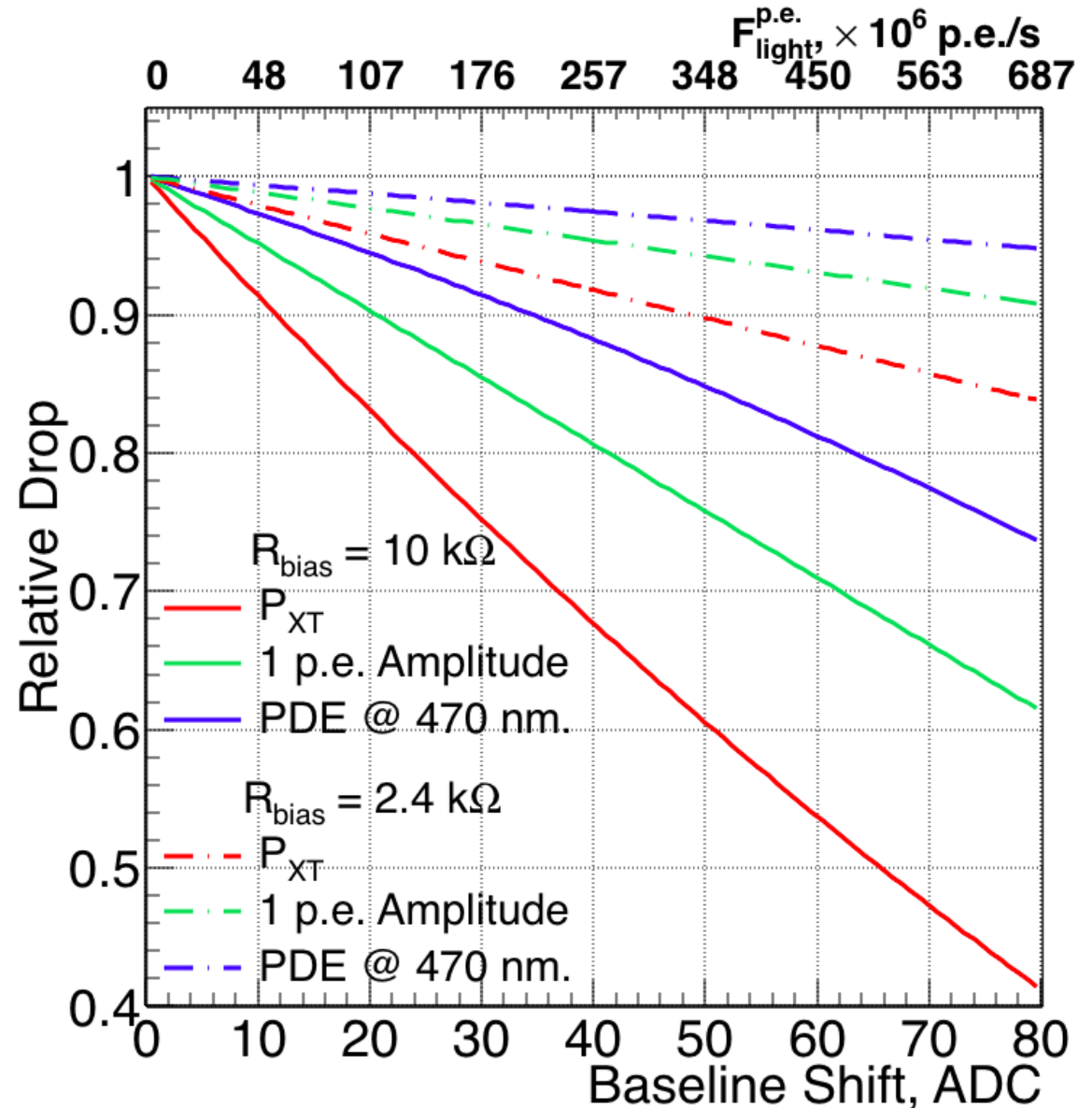


Figure 2: Typical schematics to bias SiPM device.

SiPM devices are usually biased through an RC filter to:

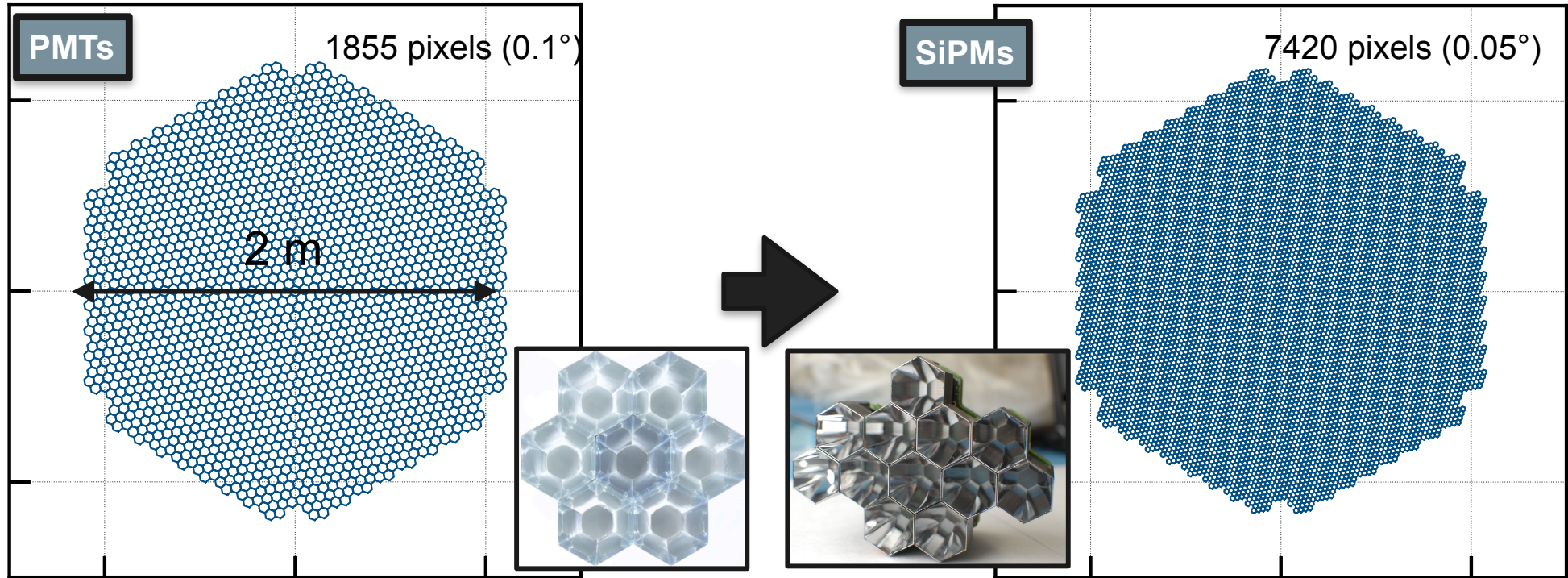
- filter high frequency electronic noise coming from the DC bias source
- limit the current to protect the sensor in case of intense illumination.
- Increase MTBF (mean time before failure) of sensor
- But this resistor induces a **voltage drop** at the sensor cathode in the presence of continuous light, which reduces the bias voltage and therefore changes its operation point



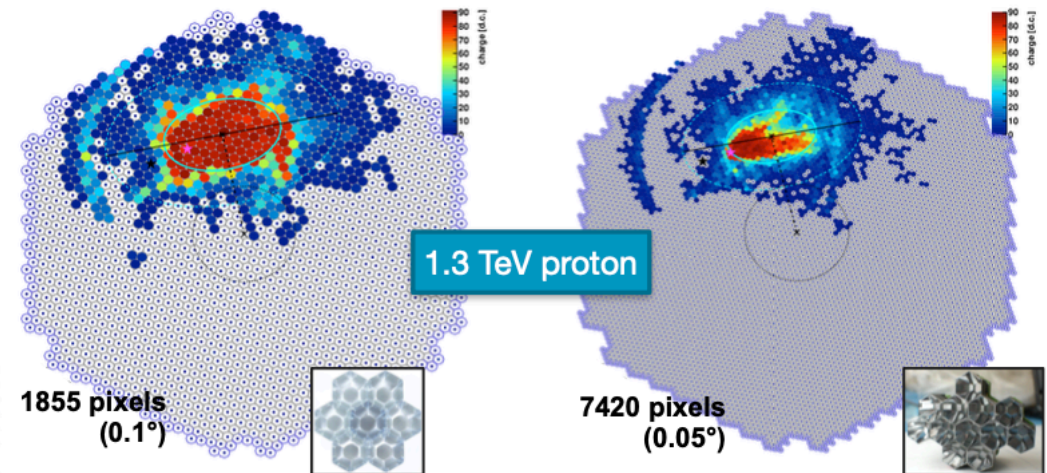
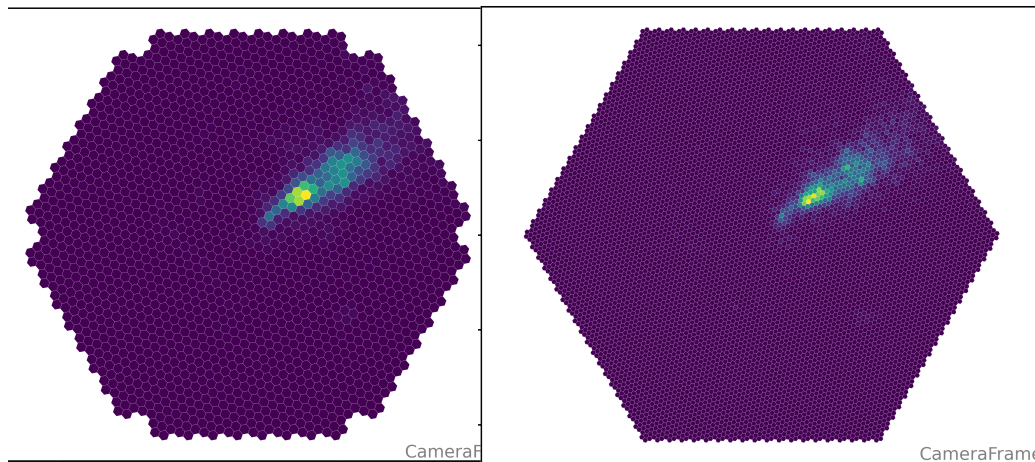
# An advanced large size telescope camera



UNIVERSITÉ  
DE GENÈVE



Gamma-ray event



## Digital Photon Counters

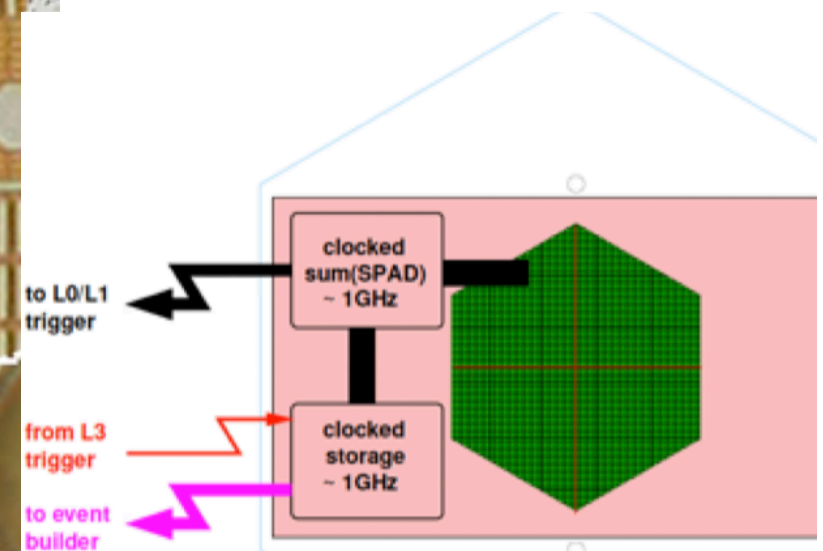
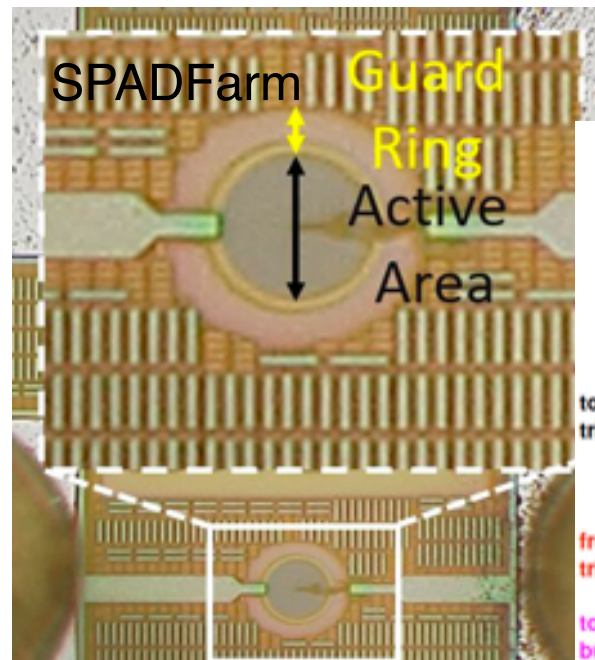
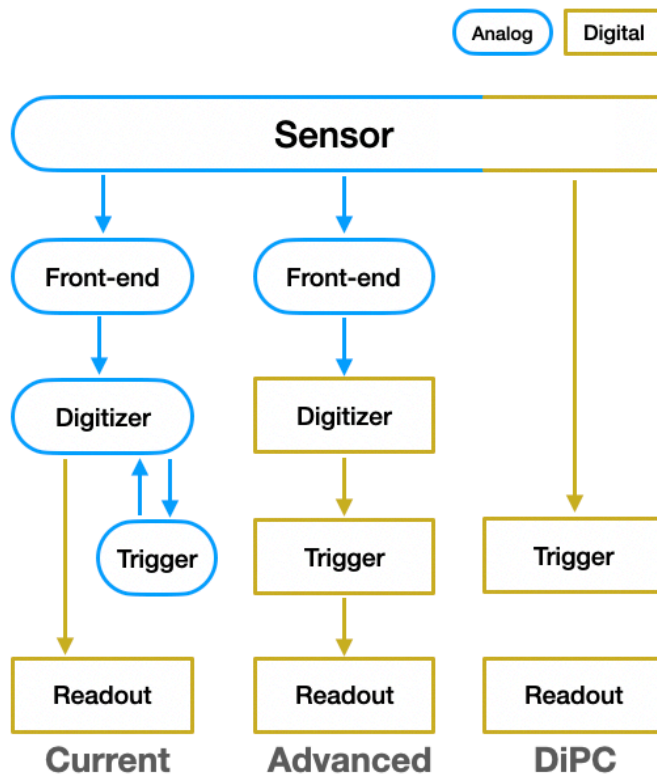
**Frontend:** Low power consumption amplification and shaping ASIC for improved SiPM technology

**Readout:** fully digital GHz readout in low power consuming ASIC.

With most of data out, real-time stereo smart triggers can be implemented. AI in ASIC or FPGAs for significant data volume reduction at raw data level as close to sensor as possible.

**Upgradable and Reprogrammable!**

- Instead of a waveform, provide a photon stream (photon count per time bin)
  - ◆ Compact and lower power photo-detection plane
- New developments based on existing SPAD technology:
  - ◆ LinoSPAD2 (CMOS 180 nm)
  - ◆ SPADFarm (CIS 110 nm)
- Data rate to output all photon information can be prohibitive, so trigger strategy on threshold+ coincidence among clusters of pixels





- SiPM are robust and have at least comparable sensitivity than PMTs
- Low-power consuming + GHz digitising + integrated AI electronics suitable for new sensors needs developments
- Digital Photon Counters are challenging due to PDE in UV but many developers undertook the challenge
- NUV detectors work well for ground and space